Electronic Supplementary Material (ESI) for ChemComm.


Electronic Supplementary Information (ESI)

# Fluorogenic Cell Surface Glycan Labelling with Fluorescence Molecular Rotor Dyes and Nucleic Acid Stains

Alen Koçak,[a] Amal K. Homer,[a] Antonia Feida,[a] Florian Telschow,[b] Jacob L. Gorenflos López,[c] Cihan Baydaroğlu,[d] Michael Gradzielski,[d] Christian P. R. Hackenberger,[a,c] Ulrike Alexiev,[b, ‡] Oliver Seitz*[a]

[a] *Department of Chemistry, Humboldt-Universität zu Berlin, Brook-Taylor-Straße 2, 12489 Berlin, Germany, E-mail: oliver.seitz@chemie.hu-berlin.de*
[b] *Institut für Experimentalphysik, Freie Universität Berlin, Arnimallee 14, 14195 Berlin, Germany*
[c] *Leibniz-Institut für Molekulare Pharmakologie, Robert-Rössle-Strasse 10, 13125 Berlin, Germany*
[d] *Institute of Chemistry, Technische Universität Berlin, Strasse des 17. Juni 124, 10623 Berlin, Germany*
‡ deceased
* corresponding author

# 1 Experimental Procedures

## 1.1 Reagents for Chemical Synthesis.

All solvents and reagents were used as received from commercial suppliers unless otherwise stated. Fmoc-protected amino acid building blocks, 6-(Fmoc-amino)hexanoic acid (Fmoc-6-Ahx-OH), (E)-2-Cyano-3-(1,2,3,5,6,7-hexahydropyrido[3,2,1-ij]quinolin-9-yl)acrylic acid (CCVJ-OH), 2-(3-(1-(5-Carboxypentyl)-3,3-dimethyl-5-sulfoindolin-2-ylidene)prop-1-en-1-yl)-1-ethyl-3,3-dimethyl-3H-indol-1-ium-5-sulfonate (Sulfo-Cyanine3-OH) was purchased from BLD Pharmatech GmbH (Kaiserslautern, Germany). 2-((1E,3E)-3-[1-(5-carboxypentyl)-3,3-dimethyl-1,3-dihydro-2H-indol-2-ylidene]-1-propenyl)-1,3,3-trimethyl-3H-indolium (Cyanine3-OH) was obtained from Lumiprobe GmbH (Hannover, Germany). TentaGel® S TRT Cl Resin was purchased from Rapp Polymere GmbH (Tübingen, Germany) with a loading of 0.22 µmol/mg. O-(1H-6-Chlorobenzotriazole-1-yl)-1,1,3,3-tetramethyluronium hexafluorophosphate (HCTU) and Ethyl (2Z)-2-cyano-2-(hydroxyimino)acetate (Oxyma) were purchased from Carbolution Chemicals GmbH (Saarbrücken, Germany). 1H-1,2,3-Benzotriazol-1-ol (HOBt) was from abcr GmbH (Karlsruhe, Germany). 4-methylbenzenesulfonate; pyridin-1-ium (PPTS) was purchased from Sigma-Aldrich Chemie GmbH (Taufkirchen, Germany). N,N-Dimethylformamide (DMF) and acetonitrile (ACN) were purchased from VWR International GmbH (Darmstadt, Germany). N,N-Diisopropylethylamine (DIPEA), N-Methylpyrrolidone (NMP) and Trifluoroacetic acid (TFA) were obtained from Carl Roth GmbH (Karlsruhe, Germany). Thiazole Orange was prepared as described [1]. Fmoc-Hydrazide was synthesized according to the literature [2].

## 1.2 Preparative HPLC

The purification of crude peptide or small molecule probes was performed on a 1100 Series HPLC system from Agilent Technologies (Santa Clara, USA) using a Polaris C18 column (5µm, 250 x 10, pore size: 220 Å) from Varian at a flow rate of 6 ml/min and a multiple wavelength detector operating at three wavelengths during the purification (λ1 = 210 nm, λ2 = 260 nm and λ3 = 280 nm). A mix of the solutions A (98.9% $H_2O$, 1.0% MeCN and 0.1% TFA) and B (98.9% MeCN, 1.0% $H_2O$ and 0.1% TFA) was used as mobile phase.

## 1.3 UPLC-MS

The purification of crude peptide or small molecule probes was performed on a 1100 Series HPLC system from Agilent Technologies (Santa Clara, USA) using a Polaris C18 column (5µm, 250 x 10, pore size: 220 Å) from Varian at a flow rate of 6 ml/min and a multiple wavelength detector operating at three wavelengths during the purification (λ1 = 210 nm, λ2 = 260 nm and λ3 = 280 nm). A mix of the solutions A (98.9% $H_2O$, 1.0% MeCN and 0.1% TFA) and B (98.9% MeCN, 1.0% $H_2O$ and 0.1% TFA) was used as mobile phase.

## 1.4 Synthesis of 3D-$N_2H_3$ backbone

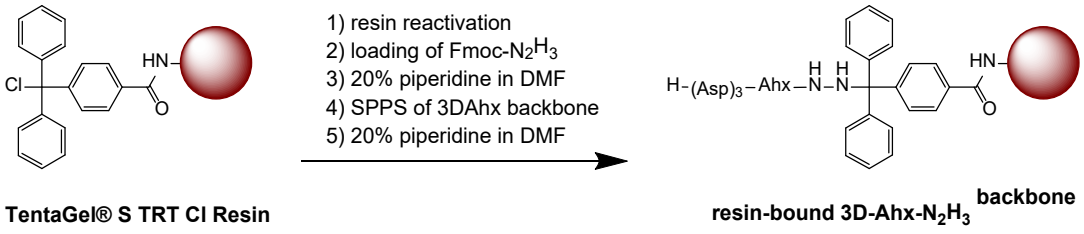


**Figure S1.** Synthesis of the 3D-$N_2H_3$ peptide backbone via Fmoc/tBu solid phase peptide synthesis strategy.

The 3D-$N_2H_3$ backbone synthesis was carried out on hydrazine functionalized TentaGel® S TRT Cl resin in a fritted syringe reactor according to the Fmoc/tBu solid phase peptide synthesis (SPPS) strategy [3, 4] on a 10 or 25 µmol scale. For this, the resin first was swollen in anhydrous dichloromethane (DCM) for 30 min and was then reactivated by treating it with 10% $SOCl_2$ (v/v) in dry DCM for 2 x 20 min at ambient temperature while shaking. Afterwards, the resin was washed 10 times with dry DCM. The resin was then functionalized using a suspension of 5 eq. Fmoc-Hydrazide with 10 eq. N,N-diisopropylethylamine (DIPEA) in dichloromethane/N,N-dimethylformamide (DMF) 1:1 (v/v) for 2 x 30 min at room temperature (RT) while shaking. Subsequently, the resin was washed thoroughly with DMF (5x), DCM (5x) and DMF (5x), was treated with 20% piperidine in DMF (3 x 3 min) to remove the Fmoc-protecting group and washed with DMF (3x).
Followed by this, 5 eq. N-alpha-(9-Fluorenylmethyloxycarbonyl)-L-aspartic acid beta-tert.-butyl ester (Fmoc-Asp(OtBu)-OH) was mixed with 4.75 eq. 1H-1,2,3-benzotriazol-1-ol (HOBt) as additive at a concentration 0.6 M in DMF/N-methylpyrrolidone (NMP) 1:1 (v/v) to which a solution of 4.75 eq. O-(1H-6-chlorobenzotriazole-1-yl)-1,1,3,3-tetramethyluronium hexafluorophosphate (HCTU) with a concentration of 0.5 M in DMF/NMP 1:1 (v/v) was added. Afterwards, the coupling mixture was activated for 5 min by adding 10 eq. DIPEA and was then immediately added to the syringe reactor. All coupling reactions were performed as single couplings for 45 min at room temp. while shaking.
Afterwards capping was performed by treating the resin with a mix of acetic anhydride: 2,6-lutidine: DMF 5:6:89 (v/v/v) for 10 min while shaking at room temp. after which the resin was washed with DMF (5x).
The last deprotection step before coupling the respective FMR was quantified photometrically at λ = 301 nm using the molar extinction coefficient of 7800 $M^{-1} \cdot cm^{-1}$.

### 1.5 Synthesis of the 3D-Ahx-$N_2H_3$ Backbone

The synthesis of the 3D-Ahx-$N_2H_3$ backbone was performed in analogy to the described procedure of the 3D-$N_2H_3$ backbone in a fritted syringe reactor on hydrazine functionalized TentaGel® S TRT Cl following the Fmoc/tBu SPPS strategy on a 10 or 25 µmol scale.

### 1.6 Coupling of FMR Dyes to the 3D-$N_2H_3$ and 3D-Ahx-$N_2H_3$ Backbones

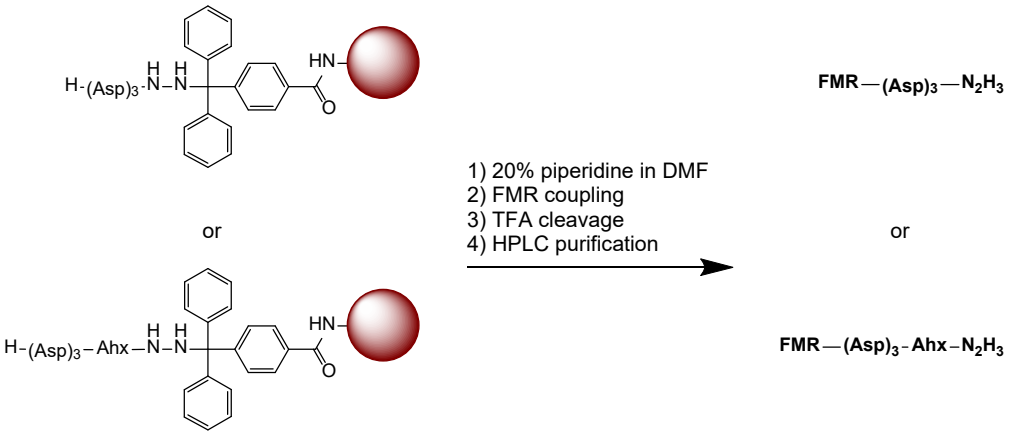


**Figure S2.** Coupling of FMR dyes CCVJ-OH, Cy3-OH or TO-OH on to the 3D-$N_2H_3$- and 3D-Ahx-$N_2H_3$ backbones via Fmoc/tBu solid phase peptide synthesis strategy, cleavage from the resin and HPLC purification.

1.5 eq. CCVJ-OH, Cy3-OH or TO-OH were coupled to the 3D-$N_2H_3$ and 3D-Ahx-$N_2H_3$ backbones on solid phase using 1.4 eq. HCTU as activating agent, 1.4 eq. HOBt as additive, 3 eq. DIPEA as base and in case of TO-OH, 1.5 eq. pyridinium para-toluenesulfonate (PPTS) in DMF/NMP 1:1 (v/v). The couplings were performed at RT while shaking for 2-3h. The resins were washed 5 times with DMF and 5 times with DCM. For the coupling of TO-OH the resins were washed with 0.6 M PPTS in DMF for 3 x 30 min. The FMR-3D-$N_2H_3$ and FMR-3D-Ahx-$N_2H_3$ probes were detached through treatment of the resin with the cleavage solution TFA/triisopropylsilane/$H_2O$ 93:3:3 (v/v/v) at room temp. for 2h. The solution was collected, the resin washed once with fresh cleavage solution for 10 min and for another 10 min in DCM. All solutions were pooled, evaporated, precipitated in ice-cold diethyl ether and centrifuged at 2000g for 30 min. The diethyl ether phase was discarded and the pellet dried using compressed air. The pellet was then resuspended in $H_2O$/acetonitrile with 0.1% trifluoracetic acid (TFA), purified by reverse-phase high performance liquid chromatography (RP-HPLC), characterized through UPLC-MS and lyophilized for 2 days prior to biological experiments (Fig. S2).

## 1.7 Synthesis of Thiazole Orange Hydrazide

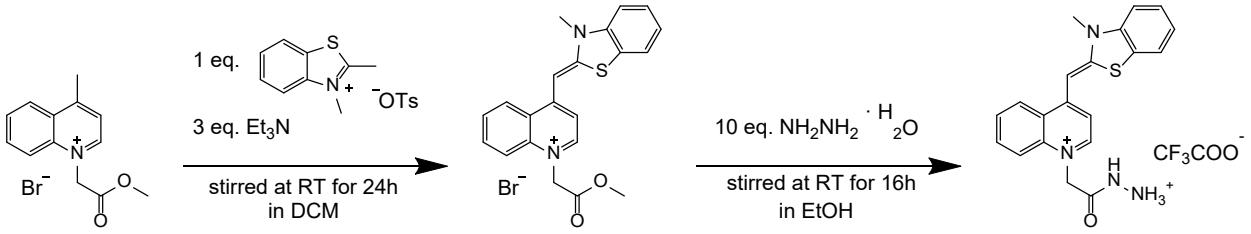


**Figure S3.** Synthesis of Thiazole orange hydrazide (TO-$N_2H_3$) in two steps starting from 1 Carbomethoxymethyl-4-methylthioquinolinium bromide.

### Thiazole orange methyl ester (TO-OMe)

Synthesis was performed by a previously established protocol.[5] 1-Carbomethoxymethyl-4-methylthioquinolinium bromide (200 mg, 0.68 mmol) and 3-methyl-2-(methylthio)- benzothiazolium tosylate (227 mg, 0.68 mmol) was dissolved in DCM (5 ml). Triethylamine (0.3 ml, 2.03mmol) was added slowly to this solution which results in immediate change of color to red. The resulting solution was allowed to stir at room temp. for 24 hours. The solid formed was collected by filtration and washed with acetone, dried in fine vacuum and used without further purification.

**Yield**: 250 mg (0.56 mmol, 83%) deep red solid, $C_{21}H_{19}N_2O_2SBr$ (443.35 g·mol−1).

**$R_t$** = 2.64 min (UPLC: 3-80% B in 4 min).

**$^1$H NMR** (300 MHz, DMSO): δ = 8.79 (d, J = 8.0 Hz, 1H), 8.48 (d, J = 7.4 Hz, 1H), 8.08 (d, J = 7.1 Hz, 1H), 7.97 – 7.90 (m, 1H), 7.85 (d, J = 8.9 Hz, 2H), 7.72 (t, J = 7.6 Hz, 1H), 7.68 – 7.60 (m, 1H), 7.52 – 7.42 (m, 2H), 7.37 (d, J = 7.3 Hz, 1H), 7.10 (d, J = 7.8 Hz, 1H), 6.99 (s, 1H), 5.60 (s, 2H), 4.07 (s, 3H), 3.77 (s, 3H).

**ESI-MS**: m/z = 363.2 (C21H19N2O2S), calcd.: 363.1.

### Thiazole orange hydrazide (TO-$N_2H_3$)

Thiazole orange methyl ester (50 mg, 0.11 mmol) was dissolved in ethanol (5 ml) in a glass vial and 22 µl (1.13 mmol) of a aqueous solution of hydrazine hydrate (64%) was added to this suspension and allowed to stir at RT for 16 hours. Ethyl acetate was added to precipitate the hydrazide and crude mixture was purified by preparative HPLC (3-80% of solvent B in 40 min).

**Yield:** 20 mg (0.042 mmol, 37%) orange powder, $C_{22}H_{20}N_4F_3O_3S$ (477.48 g·mol−1).

**Rt** = 2.16 min (UPLC: 3-80% B in 4 min).

**$^1$H NMR** (300 MHz, DMSO): δ = 8.81 (d, J = 8.4 Hz, 1H), 8.52 (d, J = 7.3 Hz, 1H), 8.09 (d, J = 8.0 Hz, 1H), 7.99 – 7.92 (m, 1H), 7.85 (d, J = 8.3 Hz, 1H), 7.75 (dd, J = 14.0, 7.7 Hz, 2H), 7.65 (t, J = 7.8 Hz, 1H), 7.51 – 7.38 (m, 2H), 7.00 (s, 1H), 5.41 (s, 2H), 4.07 (s, 3H).

**$^{13}$C NMR** (75 MHz, DMSO): δ = 165.80, 161.47, 149.15, 145.87, 140.94, 138.20, 133.70, 128.78, 127.15, 126.26, 125.32, 124.63, 124.28, 123.43, 117.83, 113.85, 107.92, 89.40, 54.71, 34.51.

**ESI-MS:** m/z = 363.3 (C20H19N4OS); calcd.: 363.1.

## 1.8 Characterization of Probes

### Thiazole orange methyl ester (TO-OMe)

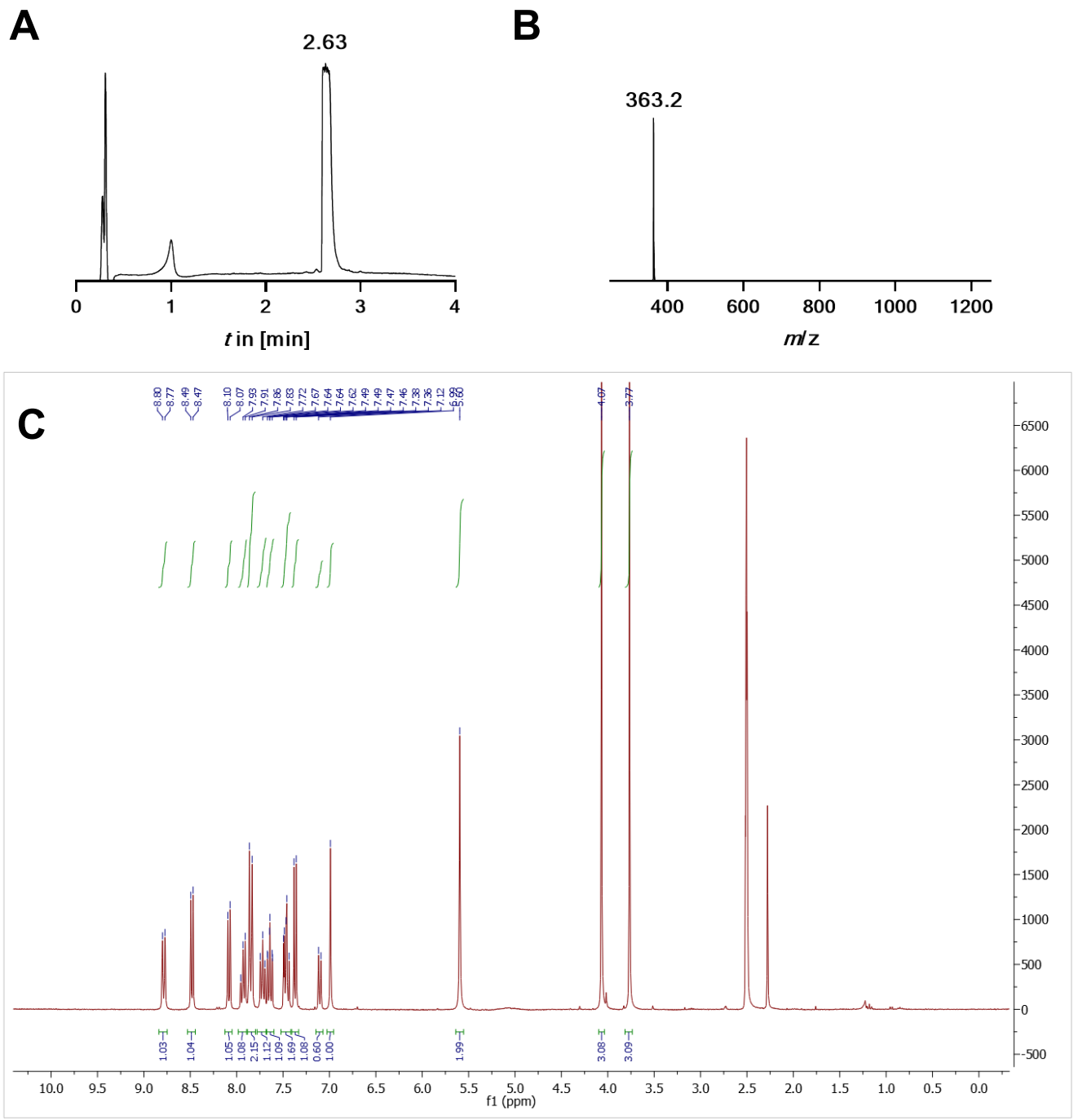


**Figure S4.** **A)** UPLC trace at λ = 260 nm (3-80% solvent B in 4 min), **B)** ESI mass spectrum from m/z = 125 - 1250 and **C)** $^{1}$H NMR (300 MHz, DMSO) for thiazole orange methyl ester (TO-OMe).

**Thiazole orange hydrazide (TO-$N_2H_3$)**

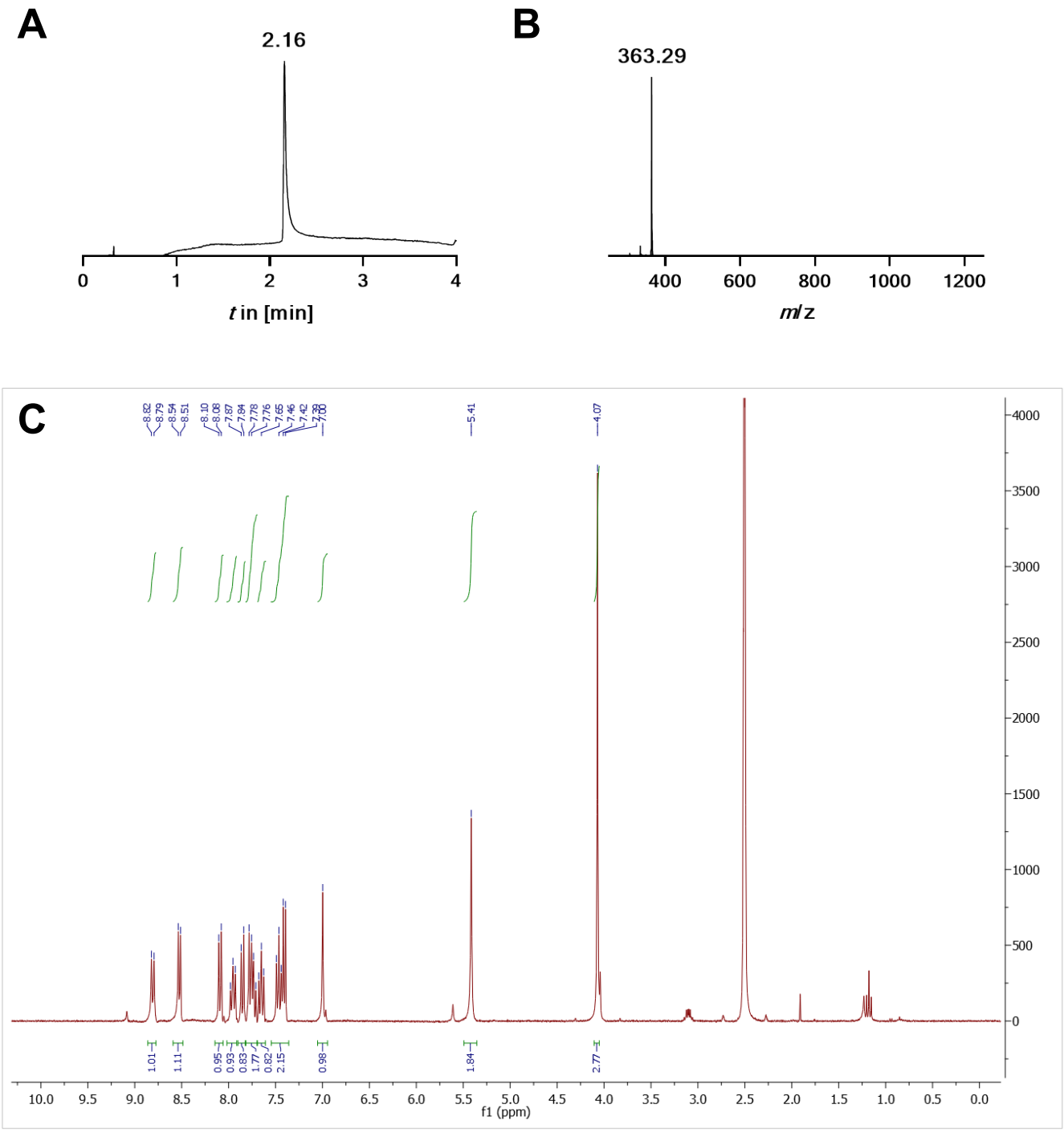


**Figure S5.** **A)** UPLC trace at λ = 260 nm (3-80% solvent B in 4 min), **B)** ESI mass spectrum from m/z = 125 - 1250 and **C)** $^1$H NMR (300 MHz, DMSO) for thiazole orange hydrazide (TO-$N_2H_3$).

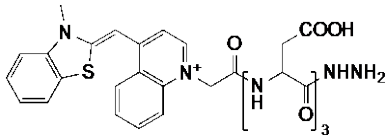

**TO-D-D-D-$N_2H_3$ (TO-3D)**

**Yield:** 43% (4.3 µmol), ε501 = 63000 $M^{-1}\cdot cm^{-1}$

**UPLC:** $t_R$ = 2.33 min (3-60% solvent B in 4 min, λ = 210 nm)

**ESI-MS:** m/z = 708.21 $(C_{32}H_{34}N_7O_{10}S)^+$; calcd.: 708.21, 354.76 $(C_{32}H_{35}N_7O_{10}S)^{2+}$ = 354.61

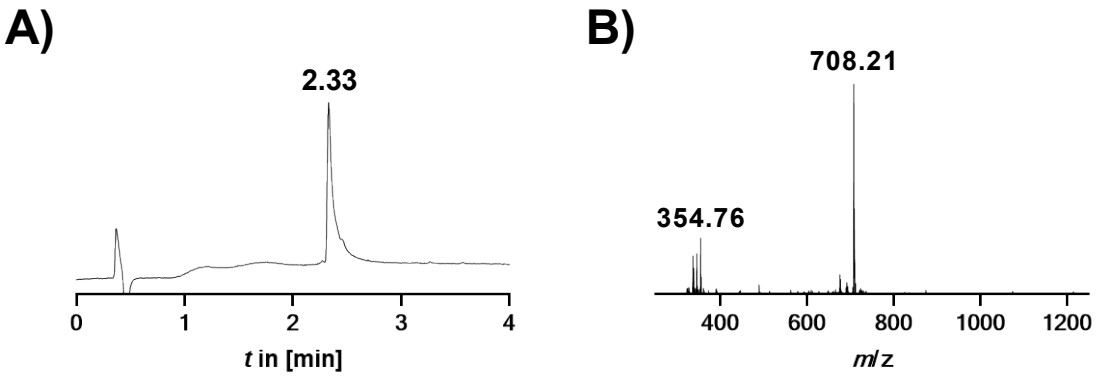


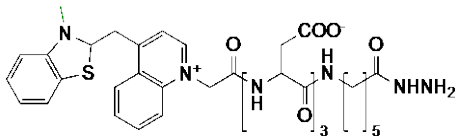

**TO-D-D-D-Ahx-$N_2H_3$ (TO-3DAhx)**

**Yield**: 51% (10.2 µmol), ε501 = 63000 $M^{-1}\cdot cm^{-1}$

**UPLC**: $t_R$ = 2.34 min (10-40% solvent B in 4 min, λ = 210 nm)

**ESI-MS**: m/z = 821.35 $(C_{38}H_{45}N_8O_{11}S)^+$; calcd.: 821.29, 411.31 $(C_{38}H_{46}N_8O_{11}S)^{2+}$ ; calcd.: 411.15

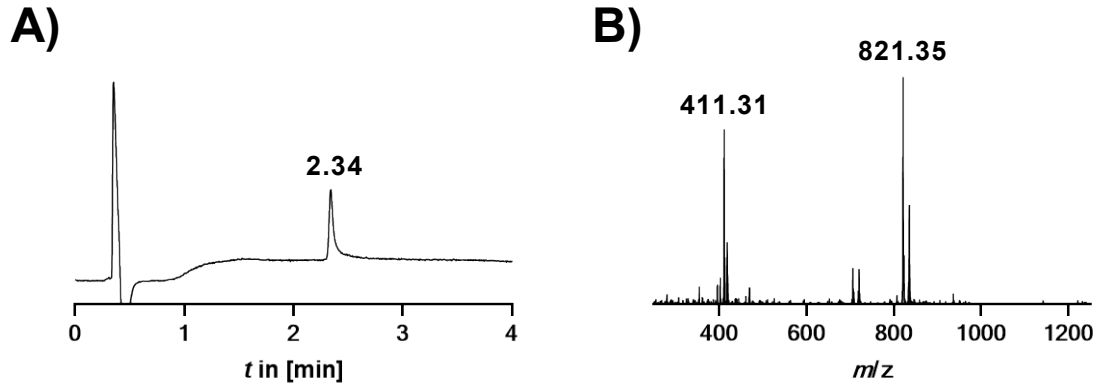

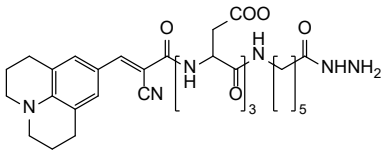

**CCVJ-D-D-D-Ahx-$N_2H_3$ (CCVJ-3DAhx)**

**Yield**: 71% (14.2 µmol), ε435 = 15500 $M^{-1}\cdot cm^{-1}$

**UPLC**: $t_R$ = 2,91 min (3-60% solvent B in 4 min, λ = 210 nm)

**ESI-MS**: m/z = 741.46 $(C_{34}H_{45}N_8O_{11})^+$; calcd: 741.32, 371.45, $(C_{34}H_{46}N_8O_{11})^{2+}$; cald.: 371.16

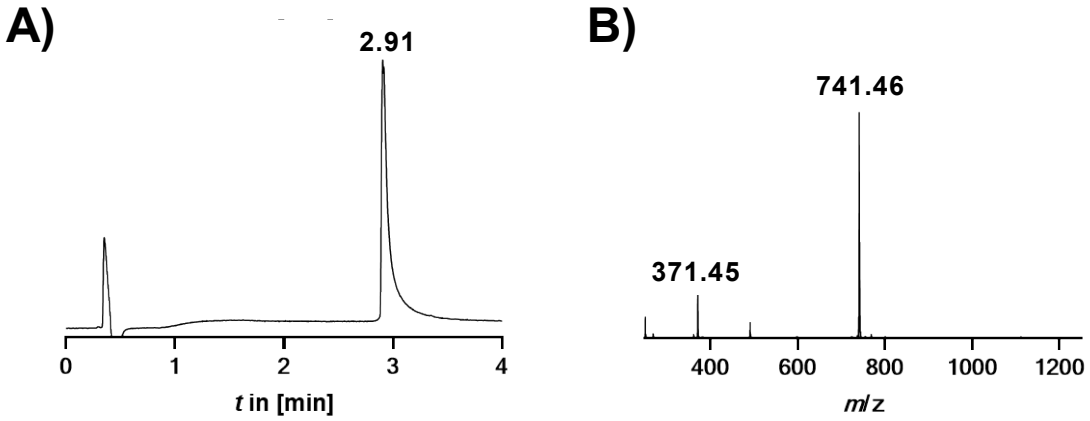


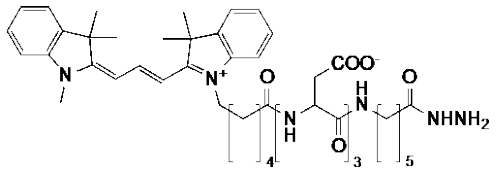

**Cy3-D-D-D-Ahx-$N_2H_3$ (Cy3-3DAhx)**

**Yield**: 81% (16.2 µmol), ε560 = 106400 $M^{-1}\cdot cm^{-1}$

**UPLC**: $t_R$ = 3.27 min (3-60% solvent B in 4 min, λ = 210 nm)

**ESI-MS**: m/z = 929.37 $(C_{48}H_{65}N_8O_{11}^+)$; calcd.: 929.48, 465.57 $(C_{48}H_{66}N_8O_{11})^{2+}$; calcd.: 465.24

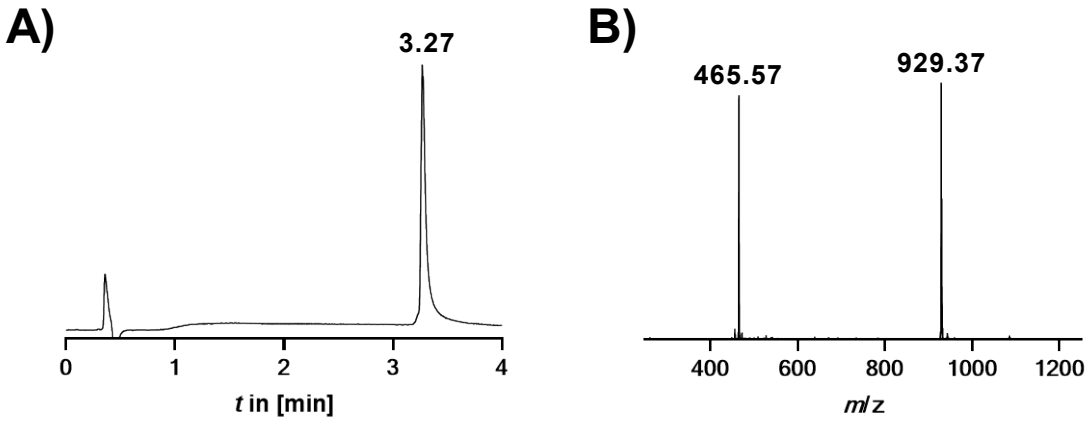

# 2 Cell Culture and Labelling Experiments

## 2.1 Reagents and Media for Cell Culture and Fluorescence Microscopy

Dulbecco's Modified Eagle medium (DMEM) High Glucose, Ham's F12 medium and RPMI 1640 medium were purchased from Biowest (Nuaillé, France). Fetal Bovine Serum (FBS), SYTOX™ Blue Dead Cell Stain, alamarBlue™ Cell Viability Reagent, StemPro™ Accutase™ Cell Dissociation Reagent, Poly-D-Lysine (0.1 mg/ml), Hoechst 33342 (10 mg/ml), Sodium meta-Periodate (NaIO4) and Alexa Fluor™ 568 Hydrazide were obtained from Thermo Fisher Scientific (Waltham, USA). Sterile 10x PBS pH 7.4 without Ca/Mg, glycerol and Tris-(2-carboxyethyl)-phosphine hydrochloride (TCEP) were purchased from Carl Roth GmbH (Karlsruhe, Germany). A549 and HeLa were obtained from ATCC (Virginia, USA). CEM cells were sourced from the research group of Prof. Dr. Frohme (TH Wildau). Sulfo-Cyanine3 hydrazide (Sulfo-Cy3, SCy3 or sulfo-Cy3-$N_2H_3$) was purchased from Lumiprobe GmbH (Hannover, Germany). Trypsin-EDTA 1X in PBS without Ca/Mg without Phenol Red was purchased from VWR International GmbH (Darmstadt, Germany). Penicillin-Streptomycin (10,000 U/mL) was obtained from MP Biomedicals Germany GmbH (Eschwege, Germany). Neuraminidase from Clostridium perfringens (C. welchii), Mucin (type II) from porcine stomach and Corning 96-well High Content Screening Microplates with Film Bottom were purchased from Sigma-Aldrich Chemie GmbH (St. Louis, USA). 5-(acetylamino)-3,5-dideoxy-3-fluoro-D-erythro-α-L-manno-2-nonulopyranosonic acid methyl ester 2,4,7,8,9-pentaacetate (P-3FAX-Neu5Ac, P3N) was purchased from Bio-Techne GmbH (Wiesbaden-Nordenstadt, Germany). FITC-SNA (Fluorescein-conjugated Sambucus Nigra Lectin was purchased from Vector Laboratories, Inc. (Newark, CA, USA). µ-Slide 8 Well microscopy slides were purchased from ibidi GmbH (Gräfelfing, Germany), cellview cell culture dishes (glass bottom with 4 compartments from Greiner Bio-One International GmbH (Kremsmünster, Austria).

## 2.2 A549 Cell Culture

A549 cells were cultured in DMEM/Hams F12 1:1 (v/v) with 10% FBS and 1% penicillin/streptomycin at 37°C and 5% $CO_2$. Once reaching 95% confluency, the supernatant medium was removed and cells were washed twice with PBS pH 7.4. Then cells were detached by incubating them for a maximum of 5 min with 1 ml Accutase at 37°C and 5% $CO_2$. To stop the Accutase activity fresh medium was added and the A549 cells were centrifuged. Lastly, the cells were resuspended in fresh medium and seeded.

## 2.3 HeLa Cell Culture

HeLa cells were cultured in DMEM supplemented with 10% FBS and 1% penicillin/streptomycin at 37°C and 5% $CO_2$. After reaching 95% confluency, the supernatant medium was removed and cells were washed twice with PBS pH 7.4. HeLa cells were detached by incubation with 0.1% trypsin/EDTA at 37°C for 3 min. Fresh medium was added to quench the trypsin activity and the cells were centrifuged. After removing the supernatant, the cells were resuspended in fresh medium and seeded.

## 2.4 CEM Cell Culture

CEM cells were cultured in RPMI supplemented with 10% FBS and 1% penicillin/streptomycin at 37°C and 5% $CO_2$. Cells were passaged once they reached 95% confluency by treating them 0.1% trypsin/EDTA at 37°C for 3 min. Following this, the cells were centrifuged, resuspended in fresh medium and seeded.

## 2.5 Fluorescence Microscopy and Image Characterizations

Widefield fluorescence microscopy experiments were performed on IX83 microscopy from Olympus using a 60x magnification lens. The channels used were:
Blue (Hoechst33342 and SYTOX Blue dead cell stain): $\lambda_{ex}$ = 350 ± 25 nm, $\lambda_{em}$ = 460 ± 25 nm; Cyan (CCVJ): $\lambda_{ex}$ =438 ± 12 nm, $\lambda_{em}$ = 483 ± 12 nm; Green/Yellow (TO and FITC): $\lambda_{ex}$ = 500 ± 12 nm $\lambda_{em}$ = 545 ± 20 nm; Red (Sulfo-Cy3, Cy3 and AF568): $\lambda_{ex}$ = 575 ± 12 nm, $\lambda_{em}$ 628 ± 20 nm.
Images were deconvoluted using the cellSens dimension software and the 2D deconvolution function. Intensity measurements, ratiometric analysis and image processing in general was performed in Fiji[6].

## 2.6 Cell Surface Labelling

Firstly, the 8-well µ-slides (ibidi, ibiTreat) were precoated with 0.05 mg/ml poly-D-lysine for 30 min at RT. Then the solution was removed, the wells were washed three times with $H_2O$ and the slides were allowed to dry. Next, 5 x $10^4$ A549 or HeLa cells were seeded per chamber and were incubated for 2 days at 37°C and 5% $CO_2$ in their respective growth medium (200 µl). For the labelling with the TO-3D-Ahx-$N_2H_3$ probe, the A549 and HeLa cells were seeded in the microscopy slide without any poly-D-lysine precoating. CEM cells (5 x $10^4$ per chamber) were always seeded on slides without additional precoating.
After 2 days, the medium was removed and the cells were gently washed three times with PBS pH 7.4 and were then treated with 1 mM $NaIO_4$ in PBS pH 7.4 for 5 min at room temp. The solution was removed, the cells were incubated for 1 min at room temp. with 1 mM glycerol in PBS pH 7.4 and washed three times with PBS pH 7.4. Depending on the utilized fluorophore, the cells were treated with 1 or 10 µM hydrazide probe together with 10 mM 5-Methoxyanthranilic acid (5MA) in PBS pH 7.4 for 5 min at room temp. and in the dark. The labelling solution was discarded and the cells were washed three times with PBS pH 7.4. Alternatively, a wash-free approach was explored with 1 µM TO-3D-Ahx-$N_2H_3$, where the cells were not washed after labelling and were instead directly imaged

(Fig. 2F). The cells were incubated with 2 µg/ml Hoechst 33342 in DMEM for 10 min at RT and were then washed thrice with PBS pH 7.4. Imaging was performed at room temp. in PBS pH 7.4 or FluoroBrite DMEM.

### 2.7 Impaired Viability of A549 Cells after Mild Oxidation and Labeling at 4°C

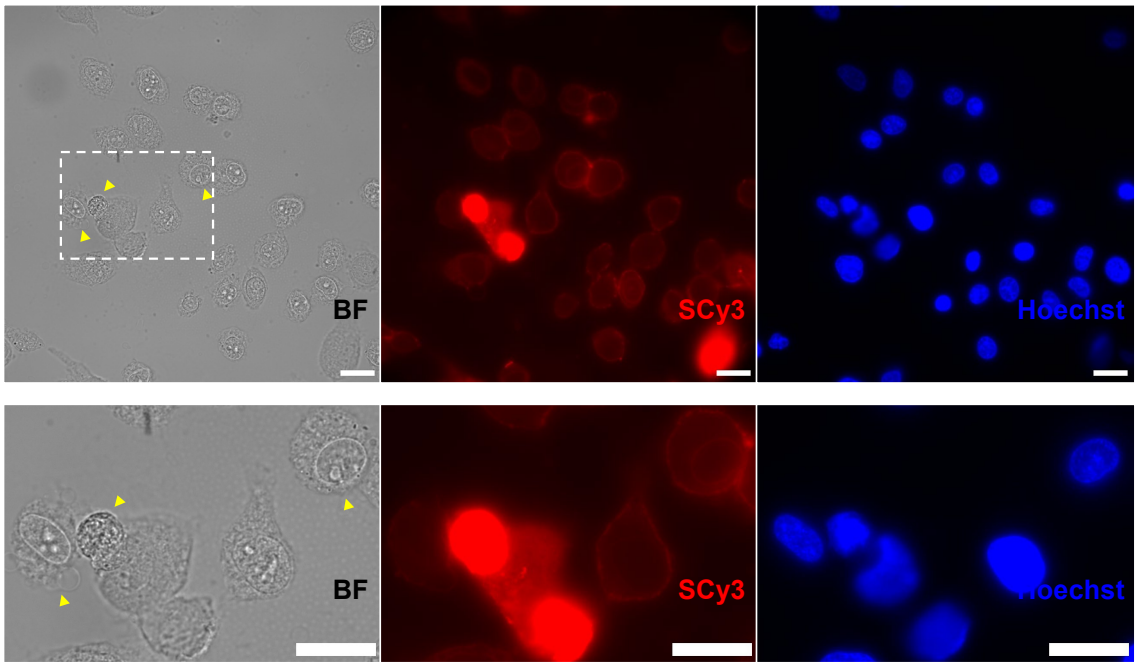


**Figure S6.** Impaired viability and altered morphology of A549 cells after being subjected to treatment with 1 mM $NaIO_4$ in PBS pH 7.4 for 30 min at 4°C followed by 10 µM sCy3-$N_2H_3$ with 10 mM aniline in PBS pH 6.9 for 30 min at 4°C. The yellow arrows highlight membrane blebbing, unusually enlarged nuclei and free-floating nuclei outside the cellular context. Scale bar = 20 µm.

### 2.8 Optimization of the Periodate-Assisted Cell Surface Labelling

Previously reported protocols relied on extended total incubation times of up to 0.5 - 2h at 4°C. [7] The cold stress can potentially cause physiological changes to the cells, specifically the periphery (Fig. S7A). To circumvent these hurdles, the labelling protocol was modified by increasing the temperature to 25°C, reducing the oxidation time with $NaIO_4$ from 30 min to 5 min and by changing the organocatalyst from previously aniline to its more reactive derivative 5-methoxyanthranilic acid (5MA) (Fig. S7B,C).[8] No labelling was observed without the sodium periodate treatment (Fig. S7D).

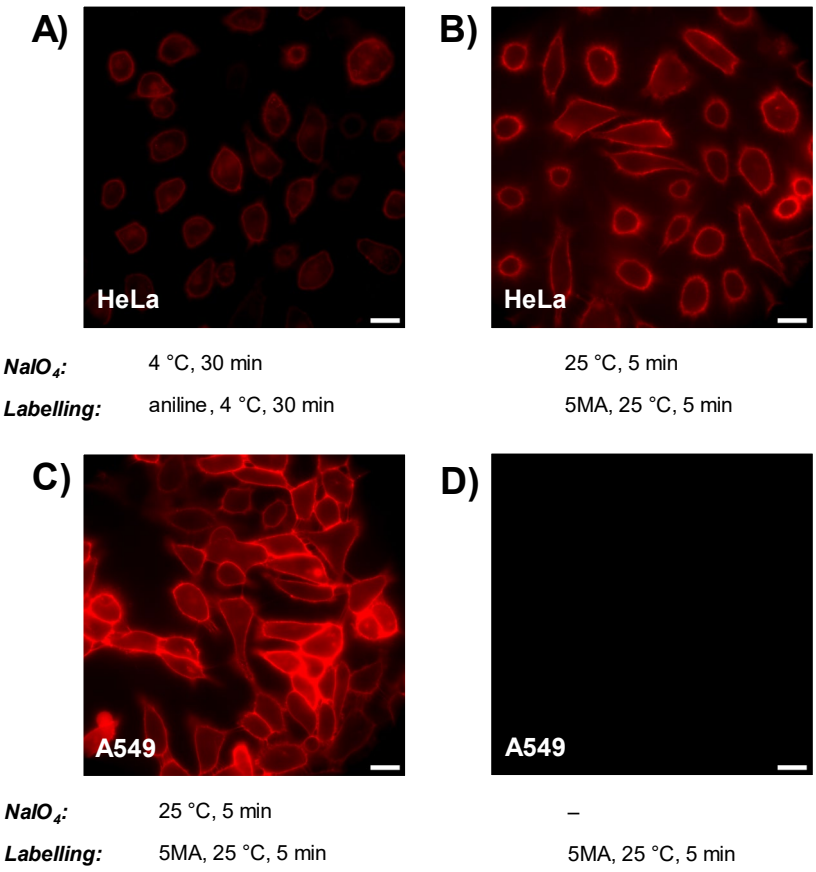


**Figure S7.** Optimization of the Periodate-Assisted Cell Surface Labelling. Fluorescent microscope images of cells incubated with Sulfo-Cy3-hydrazide (10 µM) in presence of 10 mM A) aniline, B, C) 5-methoxyanthranilic acid (5MA) and D) 5MA without prior periodate treatment. Scale bar: 20 µm.

## 2.9 Designing a Universally Applicable Probe Scaffold

Initial experiments with TO-$N_2H_3$ resulted in only poor cell surface labeling and mainly exhibited intracellular staining. To bypass excessive cellular uptake, TO was attached to a triaspartate peptide hydrazide through solid phase peptide synthesis. TO-3D-$N_2H_3$ provided rather weak signals at both the surface and, in punctuate form, inside the cells. Motivated by the weak but distinct surface staining, we investigated the incorporation of flexible spacers at the C-terminus and between TO and the anionic peptide moiety. The best results were obtained with TO-3D-Ahx-$N_2H_3$, which contained an aminohexanoyl (Ahx) linker at the C-terminus (Fig. 2C, D).

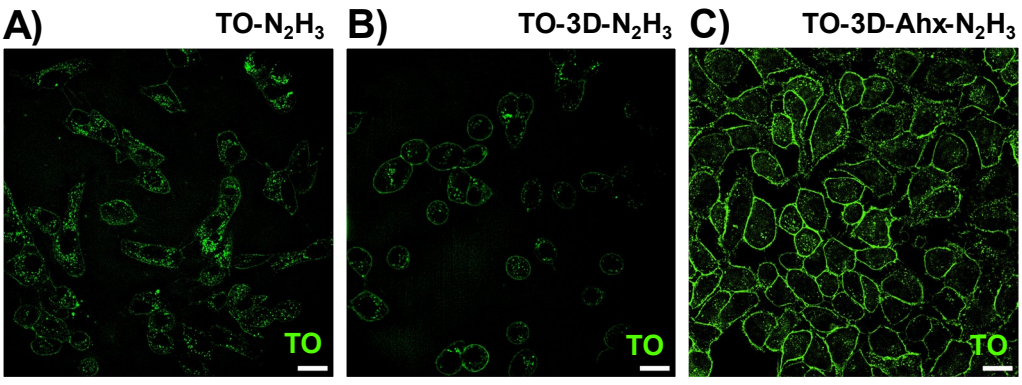


**Figure S8.** Design approach for a universally applicable peptidic probe scaffold. Fluorescence microscope images of A549 cells labelled with A) 0.1 µM TO- $N_2H_3$, B) 1 µM TO-3D- $N_2H_3$and C) 10 µM TO-3D-Ahx- $N_2H_3$. Conditions: *I.* 1 mM $NaIO_4$ in PBS pH 7.4, 5 min, 25°C, *II.* hydrazide probe, 10 mM 5MA in PBS pH 7.4, 5 min, 25°C. Scale bar: 20 µm.

## 2.10 Control Experiments for Cell Surface Labelling using FMR-3D-Ahx-$N_2H_3$ probes

TO-, CCVJ- and Cy3-3D-Ahx-$N_2H_3$ were tested on A549 cells without previous $NaIO_4$ treatment as well as in the absence of the catalyst 5MA. In addition, the cells were tested for auto-emission by applying channels and settings used in Figure 1 (Fig. S9).

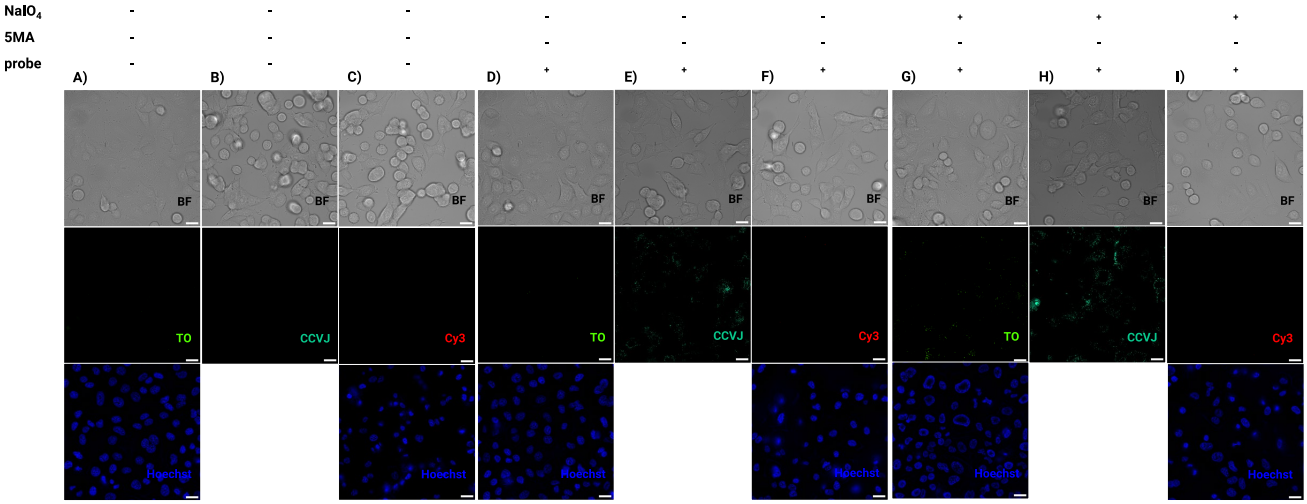


**Figure S9.** Micrographs for control experiments using TO-, CCVJ- and Cy3-3D-Ahx-$N_2H_3$ on A549 cells. The auto-emission in the according channels with the same settings was recorded without $NaIO_4$-treatment and in the absence of probe **(A-C)**. Unspecific uptake/labelling was tested by adding the respective probes to cells without prior sodium periodate incubation **(D-F)**. The requirement for the catalyst 5MA was tested in panels **(G-I)**. Scale bars = 20 µm.

## 2.11 Cell Viability after 5MA-Catalyzed Labelling of A549 Cells

A549 cells were treated accordingly with the above method at room temperature. Subsequently, the cell viability was characterized using the SYTOX Blue Dead Stain (75 nM in DMEM at 25°C for 10 min) in comparison to a positive control of A549 cells which were treated with 70% EtOH for 1 min at 25°C (Fig. S7).

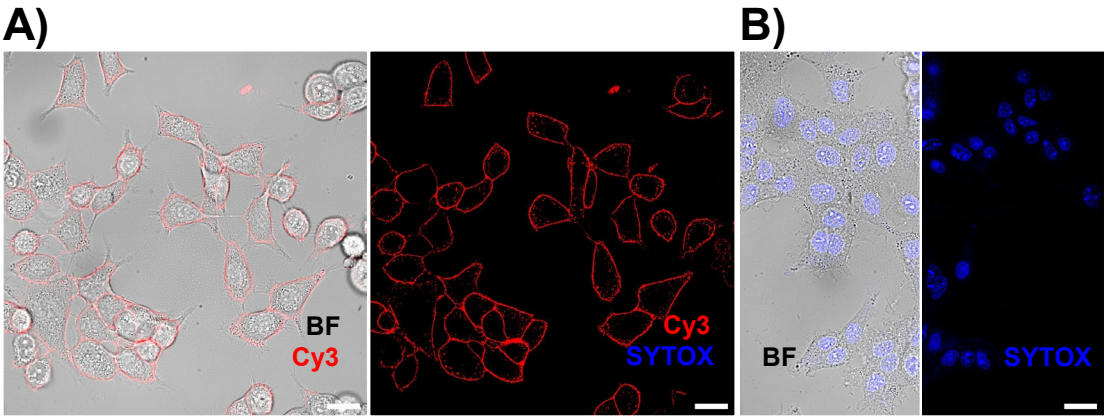


**Figure S10.** Cell viability after mild oxidation followed by 5MA-catalysed labelling with sCy3-$N_2H_3$ was characterized with SYTOX Blue Dead Cell Stain (blue) **A)** in comparison to **B)** a positive control involving treatment of A549 cells with 70 % EtOH. Left images show overlays of bright field and fluorescence microscopy images in sCy3 and SYTOX channels. Scale bar = 20 µm.

Additionally, the cell viability was assessed via alamarBlue assay (Thermo Fisher Scientific (Waltham, USA)) following the manufacturer documentation. 5 x $10^4$ A549 were seeded in a 96-well plate and were incubated for 48h at 37°C and 5% $CO_2$. Cells were then washed with PBS pH 7.4 (3x) and were subjected to either treatment with only $NaIO_4$ (Fig. S8A), 5MA (Fig. S8B) or consecutively with both NaIO4 and 5MA (Fig. S8C). Afterwards, the cells were incubated for 4h in growth medium (DMEM/Hams F12 1:1 (v/v) with 10% FBS) with 10% alamarBlue reagent at 37°C and 5% $CO_2$. The absorption values of the samples were then measured in a VICTOR3™ Multilabel Plate Reader (PerkinElmer GmbH (Waltham, USA)) at 570 and 600 nm.

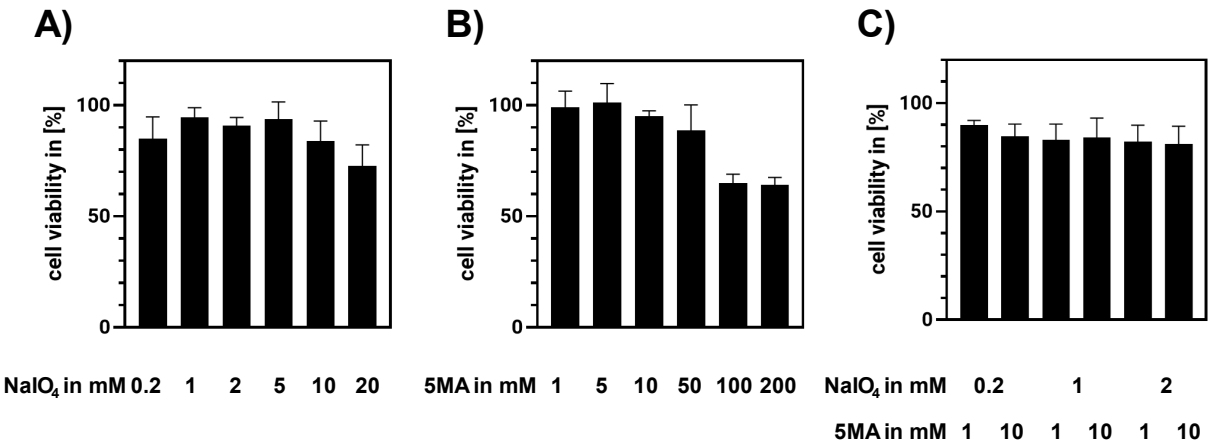


**Figure S11.** AlamarBlue assay for the characterization of the viability of A549 cells after treatment with **A)** only $NaIO_4$, **B)** only 5MA or first **C)** $NaIO_4$ and then 5MA.

## 2.12 Applying 5MA-Catalyzed Labelling on HeLa and CEM Cells

In analogy to A549 cells, HeLa (Fig. S9A-C) and CEM cells (Fig. S9D-F) were oxidized for 5 min at 25°C with 1 mM NaIO4 in PBS pH 7.4 and were then subjected to 1 µM AF568- or 10 µM CCVJ-, TO-, or Cy3-3D-Ahx-$N_2H_3$ probe together with 10 mM 5MA in PBS pH 7.4 for 5 min at 25°C (Fig. S9).

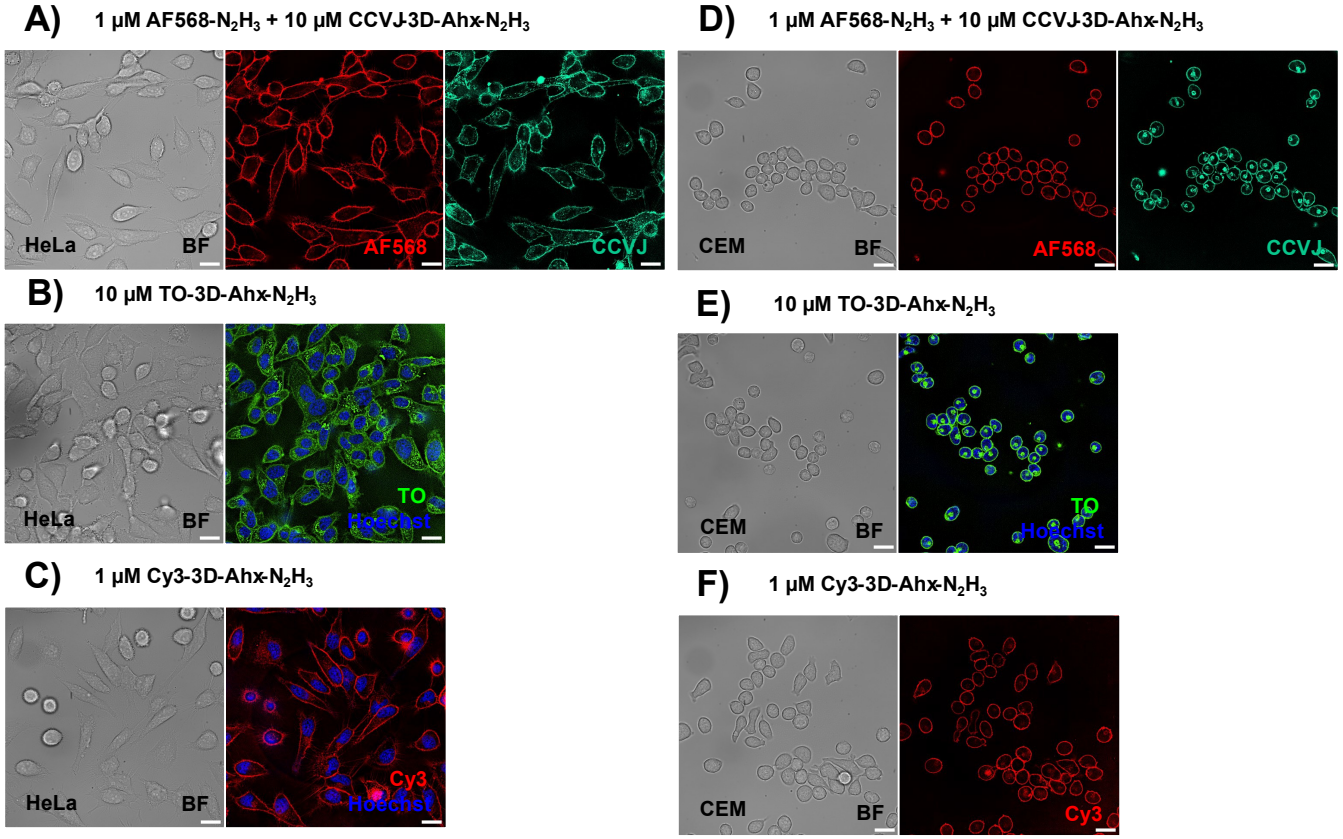


**Figure S12.** Surface labelling by 5MA-catalyzed acylhydrazone ligation of **A)-C)** HeLa and **D)-F)** CEM cells with **A)**, **D)** a combination of probes or **B)**, **C)**, **E)**, **F)** single probes. Scale bar = 20 µm.

## 2.13 Specificity Assessment of Labelling

The specificity assessment of the employed cell surface labelling method was performed on a TECAN Spark Cyto plate reader with an integrated widefield fluorescence microscope with 10x lens. The following channels were used for fluorescence measurements as well as fluorescence imaging:
Blue (Hoechst33342): $\lambda_{ex}$ = 381 - 400 nm, $\lambda_{em}$ = 414 – 450 nm; Green (FITC): $\lambda_{ex}$ = 461 – 487 nm, $\lambda_{em}$ = 500 - 530 nm; Red (Sulfo-Cy3): $\lambda_{ex}$ = 543 – 566 nm, $\lambda_{em}$ 580 – 611 nm.
Images were processed and cells were segmented automatically with the Image Analyzer software. Cells were detected in the blue channel based on the Hoechst33342 stained nuclei and regions of interest (ROI) were defined per cell (Fig. S10A, B + E, F). The detected fluorescence intensities for the red (Fig. S10A, B) and green channel (Fig. S10E, F) were quantified as green or red fluorescent intensity per blue object count.
As expected, the staining intensity per cell correlated with the applied concentration of sCy3 dye. Incubation of cells for 45 min with NA (0.4 U/ml) from Clostridium perfringens in DMEM at 37°C induced a marked reduction of signal by approx. 30 % (Fig. S10 C). In comparison, a 20 % signal reduction was achieved with FITC-SNA (Fig. S10 G). Interestingly, the FITC-SNA signal was further reduced by about 45 % when the cells were treated with sodium periodate after neuraminidase incubation suggesting that enzymatic cleavage of sialic acid residues was not quantitative. Staining by both sCy3-$N_2H_3$ and FITC-SNA was reduced respectively by 25% and 45% when the cells were incubated for 48 h with 100 µM sialyltransferase inhibitor P-3FAX-Neu5Ac (P3N) in DMEM/Ham's F12 with 10% FBS at 37°C for 48 h prior to labelling (Fig. S10D, H). The results suggest that a 5 min periodate treatment at room temperature still provides sialic acid selectivity.

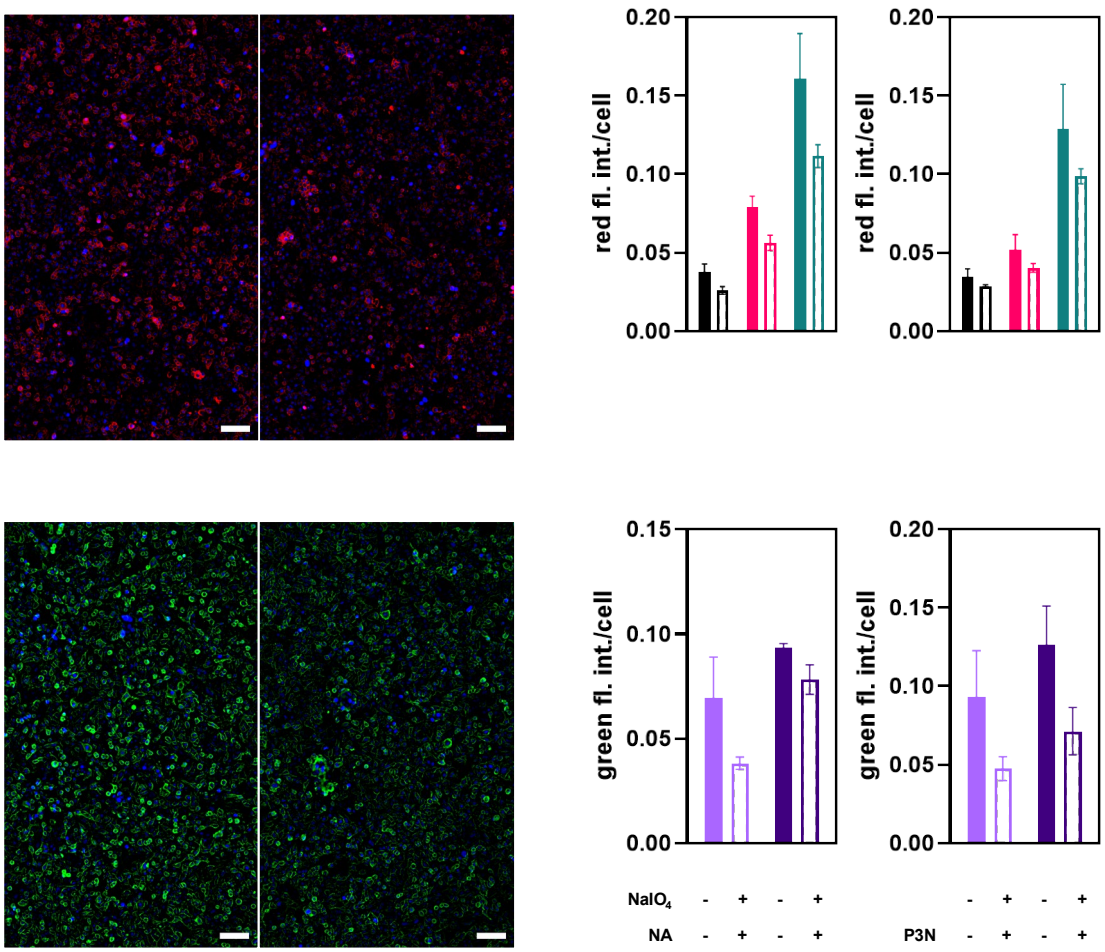


**Figure S13.** Specificity assessment of periodate-assisted and 5MA-catalyzed cell surface labelling onA549. **A)** Cells were labelled with the sialic acid specific FITC-SNA as a control and fluorescence was imaged in the green channel. **B)** A549 cells were treated with 1 mM $NaIO_4$ in PBS pH 7.4 for 5 min at 25°C and were then labelled with 10 µM sCy3-$N_2H_3$. The left panels in **A+B)** show cells that were not subjected to a neuraminidase (NA) from *Clostridium perfringens* treatment prior to labelling whereas cells in the right panels were incubated with 0.4 mg/ml NA in DMEM at 37°C for 45 min. Scale bar = 100 µm. Conditions: see 3.6 for labelling with sCy3-$N_2H_3$; nuclear stain: 2 µg/ml Hoechst33342 in DMEM for 10 min at 25°C.

## 3 Ratiometric Analysis of Fluorescence Microscopy Images

Multi-channel stack images of cells labelled with AF568-$N_2H_3$in combination with TO – or CCVJ-3D-Ahx-$N_2H_3$ (channel 1: brightfield, channel 2: red (AF568), channel 3: cyan (CCVJ-3D-Ahx-$N_2H_3$) or green (TO-3D-Ahx-$N_2H_3$) and channel 4: blue (Hoechst33343) were processed, segmented and ratiometrically analysed using Fiji running on ImageJ 1.54f [6] in combination with TrackMate [9, 10] and Cellpose [11]. Two scripts were developed to semi-automate the process. The first script duplicates the current stack creating a new stack with only channel 2 and 3, applies the rolling ball background subtraction algorithm with a radius of 50 pixels in both channels, automatically adjusts the contrasts and finally starts the Trackmate plugin integrated with Cellpose (Script 1).

```
run("Duplicate...", "duplicate channels=2-3");
     Stack.setChannel(1);
          run("Subtract Background...", "rolling=50 stack");
     Stack.setChannel(1);
          run("Enhance Contrast", "saturated=0.35");
     Stack.setChannel(2);
          run("Enhance Contrast", "saturated=0.35");
     Stack.setChannel(1);
          run("TrackMate");

```

**Script 1.** Duplicates the multi-channel image comprising only the channels 2 and 3, applies the rolling ball background subtraction with a radius of 50 px, automatically adjusts the contrasts and starts the Trackmate plugin.

Followed by this the cells were automatically detected and segmented in Trackmate powered by the Cellpose algorithm (Fig. S11B). The resulting approximately circular ROIs were then transformed into donut shapes comprising only the cell surface without the cytoplasm (Fig. S11C). This ensured that only cell surface resident pixels were considered for the ratiometric analysis (Script 2).

```
// Make sure the ROI Manager is open
if (isOpen("ROI Manager") == 0) {
    run("ROI Manager...");
}

// Count the number of ROIs
n = roiManager("count");

// Process each ROI
for (i = 0; i < n; i++) {

    // Select the current ROI
    roiManager("Select", i);

    // Create outer periphery
    run("Enlarge...", "enlarge=10 pixel");
    // Adjust this pixel value as needed
    roiManager("Add");

    // Return to the initial ROI
    roiManager("Select", i);

    // Create inner periphery
    run("Enlarge...", "enlarge=-20 pixel");
    // Adjust this pixel value as needed
    roiManager("Add");

     ni = roiManager("count");

    // Subtract inner from outer to get periphery
    roiManager("Select", newArray(ni-1,ni-2));
    roiManager("AND");
    roiManager("XOR");
    roiManager("Add");

}

roiManager("Show All with labels");
n = roiManager("count");

for (i = n-1; i >= 0; i--) {
    roiManager("Select", i);
    name = Roi.getName();
    if (lengthOf(name) <7) {
        roiManager("Delete");
    }
}
```

**Script 2.** Transforms each automatically created ROI into a donut shaped ROI that mainly includes the cell surface leaving out the cytoplasm.

Lastly, the original channel 3 (FMR-labelled) was divided by channel 2 (non-FMR-labelled) using the integrated Image Calculator module (Fig. S11D). The beforehand created ring-shaped regions of interest were applied onto the ratiometric images and the IFMR/Inon-FMR fluorescence intensities ratios were readout directly per cells (Fig. S11E).

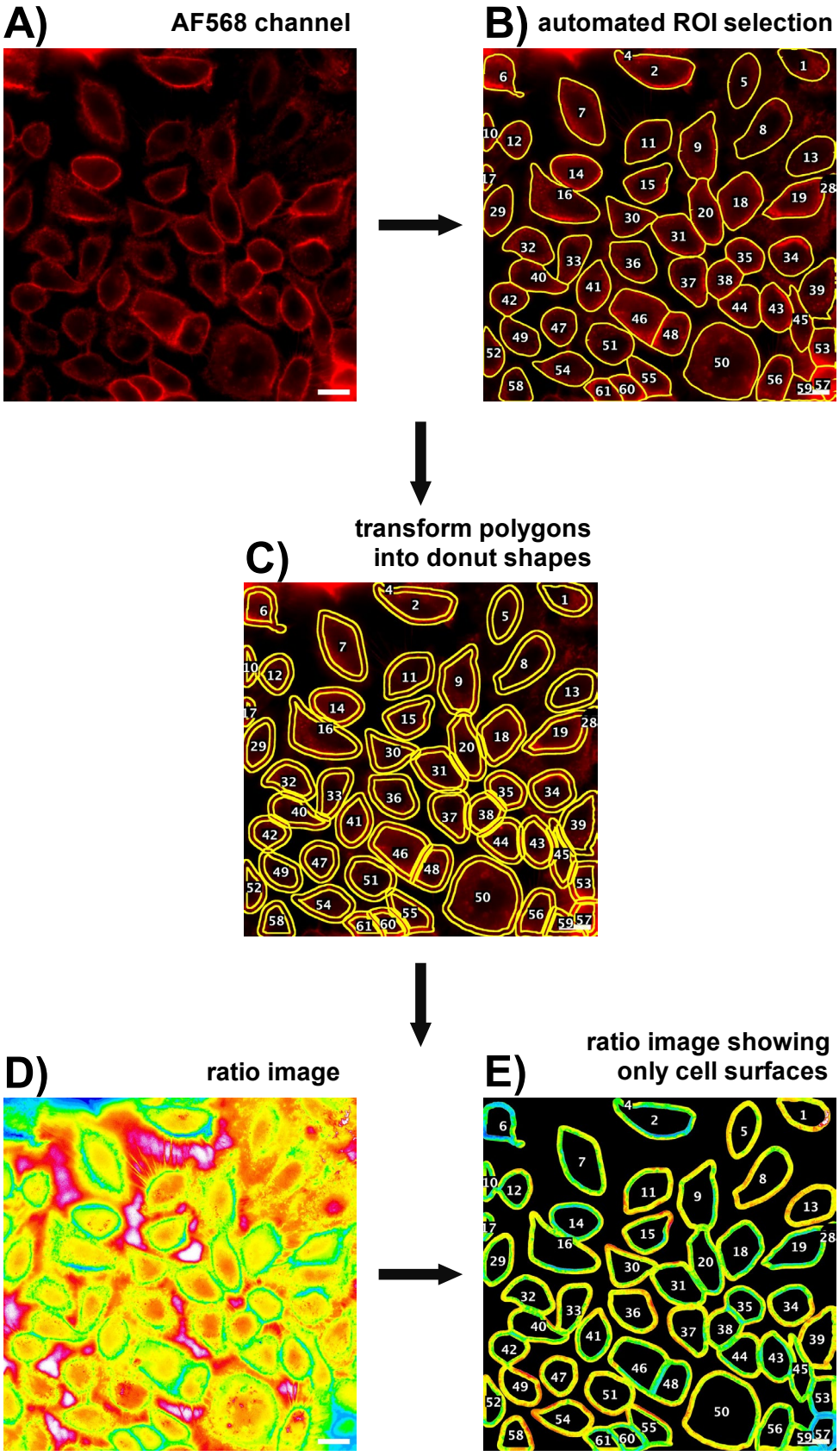


**Figure S14.** Process of creating ratio images. The **A)** AF568 channel was used for the **B)** automated cell detection using TrackMate and Cellpose in Fiji and **C)** transforming the polygons into donut shapes. The **D)** ratio image (here TO/AF568) were created from the original AF568 – and TO-images without any background correction or thresholding. **E)** The donut shaped ROIs were overlayed onto the ratio image and the outside of the selections was cleared resulting in black background and cytoplasmic lumens. Scale bar: 20 µm.

### 3.1 Characterization of Alexa Fluor 568 Fluorescence Spectrum in Viscous Medium

Possible viscosity-dependencies of Alexa Fluor 568 (AF568) were examined by measuring the fluorescence spectrum of 0.5 µM AF568-$N_2H_3$ in PBS pH 7.4 as well as in 80% glycerol in PBS pH 7.4 (Fig.S12).

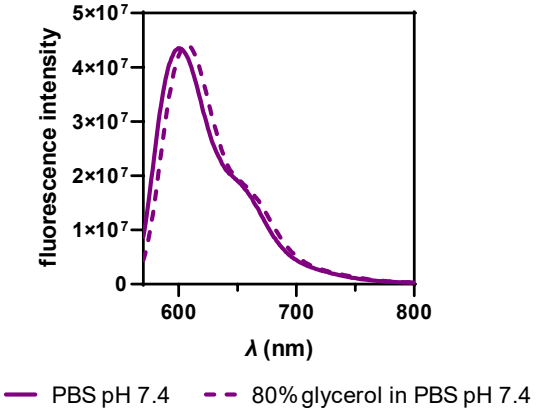


**Figure S15.** Fluorescence spectrum of 0.5 µM AF568-$N_2H_3$ in PBS pH 7.4 and in 80% glycerol in PBS pH 7.4. The spectrum of AF568 was background corrected with the blank PBS pH 7.4 spectrum.

## 4 Labelling Mucin from Porcine Stomach

A 2% (w/v) (20 mg/ml) solution of type II mucin from porcine stomach was prepared in PBS pH 7.4. The mucin solution was gently stirred overnight at ambient. Centrifugation steps throughout the handling of mucin were performed at 5000 x g for 5 min at 25°C when the mucin samples were in microtubes (1.5 or 2 ml) or at 2000 x g for 5 min at 25°C when the solution was in larger vessels. The mucin was then gently washed three times with PBS pH 7.4 to remove possible impurities before any experiment.
Subsequently, the mucin samples were treated with 1 mM NaIO4 in PBS pH 7.4 for 30 min at 37°C while shaking at 200 rpm every 30 seconds for 30 seconds. Then the sodium periodate solution was removed and the samples were first washed once with 1 mM glycerol in PBS pH 7.4 and then twice with PBS pH 7.4. Following this 10 µM TO – or CCVJ-3D-Ahx-$N_2H_3$ together with 10 mM 5MA in PBS pH 7.4 were incubated on the individual resin samples for 30 min at 37°C while shaking gently. Mucin samples were then treated with 1 and 10 mM TCEP in PBS pH 7.4 for 30 min at 37°C while shaking. A negative control without TCEP was incubated for the same time in PBS pH 7.4. Blank mucin controls were prepared by treating mucin with periodate without subsequent hydrazone labelling. Before measurements, the respective mucin sample was concentrated from 2% (w/v) to final concentration of 8% (w/v) by centrifugation and resuspending the sample in a quarter of the previous volume of PBS pH 7.4.

### 4.1 Fluorescence Intensity Measurements

Fluorescence intensity measurements were performed using Hellma Ultra-Micro cell cuvette (optical path length = 10 mm, aperture = 5 x 2 mm and volume = 100 µl) on a SPEX Fluoromax 3 fluorescence spectrometer (HORIBA Jobin Yvon) equipped with a peltier thermostated single cell holder (set to 25 °C). Wavelengths used for samples with TO-3D-Ahx-N2H3 were: $\lambda_{ex}$ = 460 nm, $\lambda_{em}$ = 470 – 800 nm, for CCVJ-3D-Ahx-N2H3: $\lambda_{ex}$ = 435 nm, $\lambda_{em}$ = 445 – 800 nm and for AF568-N2H3: $\lambda_{ex}$ = 560 nm, $\lambda_{em}$ = 570 – 800 nm. The fluorescence spectra of blank mucin controls were subtracted from the fluorescence spectra of labelled mucin.

### 4.2 Characterization of CCVJ-OH in porcine mucin solution

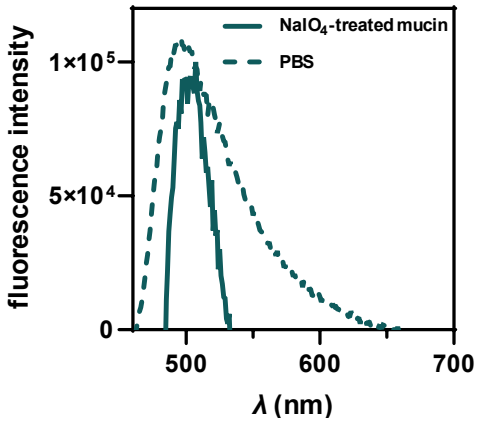


**Figure S16.** Fluorescence spectrum of 10 µM CCVJ-OH in PBS pH 7.4 and in $NaIO_4$-activated porcine stomach mucin (8% w/v). Spectra were background corrected by subtracting a blank solution spectrum from the corresponding raw spectrum.

### 4.3 Characterization of Cy3-3D-Ahx-$N_2H_3$ on porcine mucin and in solution

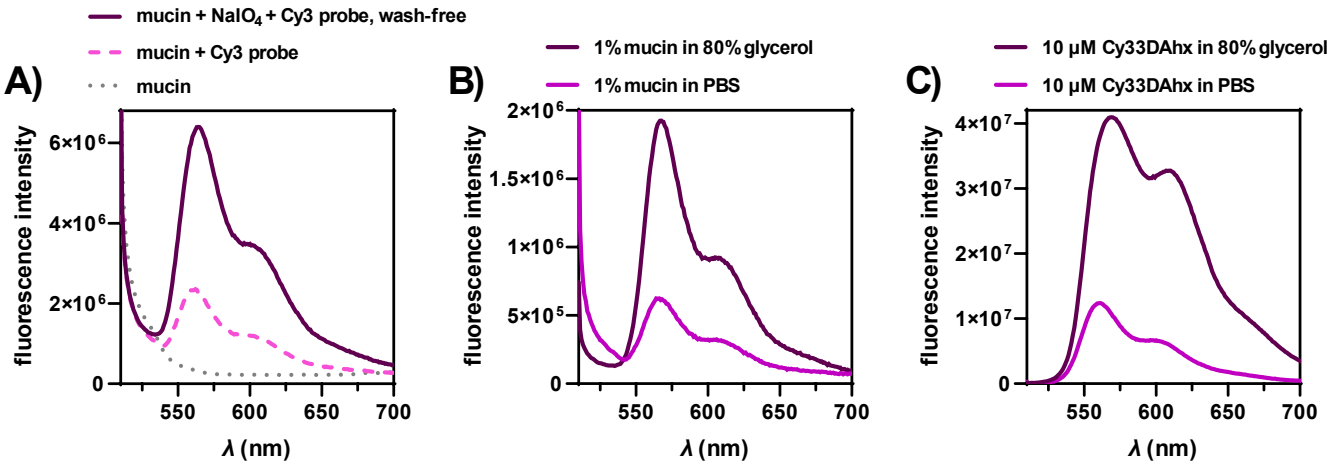


**Figure S17.** Fluorescence spectra of **A)** mucin (8% w/v) with or without sodium periodate treatment labelled with Cy3-3D-Ahx-$N_2H_3$, **B)** mucin (1% w/v) labelled with Cy3-3D-Ahx-$N_2H_3$ and resuspended in either PBS or 80% glycerol and **C)** 10 µM Cy3-3D-Ahx-$N_2H_3$ in PBS pH 7.4 and 80% glycerol.

### 4.4 Characterization of Fluorescence Spectra in the Presence of TCEP

To assess potential chemical quenching of fluorescence, TO – and CCVJ-3D-Ahx-$N_2H_3$ were dissolved at 1 µM concentration in 80% glycerol in PBS. Fluorescence spectra were measured before and after incubation with 10 mM TCEP in 80% glycerol in PBS for 1h at 37°C (Fig. S11).

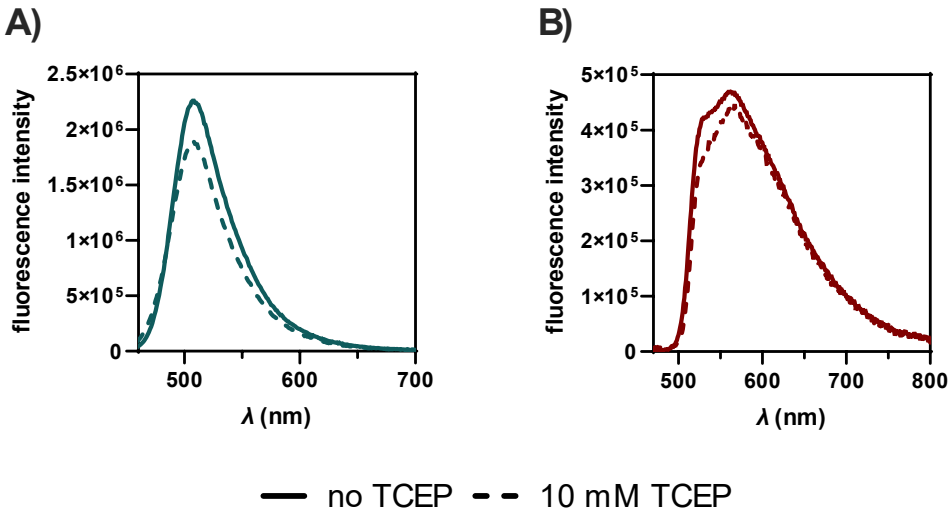


**Figure S18.** Fluorescence spectra of **A)** CCVJ-3D-Ahx-$N_2H_3$ and **B)** TO-3D-Ahx-$N_2H_3$ in 80% glycerol in PBS before and after incubation in 10 mM TCEP for 1h at 37°C. Spectra were background corrected by subtracting a blank solution spectrum from the corresponding raw spectrum.

### 4.5 Rheological characterization of porcine stomach mucin

The Anton Paar MCR 502 WESP rheometer was used as the measuring instrument and the cone-plate system as the measuring unit, with CP-25 being selected as the cone. Before the measurements were started, the Peltier element was brought to the desired temperature. First, an amplitude sweep was performed covering a range of shear deformation γ between 0.01-10% at a constant frequency 1 rad/s to determine the linear viscoelastic (LVE) region. Subsequently a frequency sweep between 0.1 and 100 rad/s was conducted, with a fixed shear deformation at 2% (for all TCEP-treated samples) and 0.7% for the untreated negative control. All measurements were performed at both 25 °C, up (0.1-100 rad/s) and down (100 to 0.1 rad/s) respectively. Further, the data were analyzed with regards to the storage modulus G' (Pa) and the loss modulus G'' (Pa).

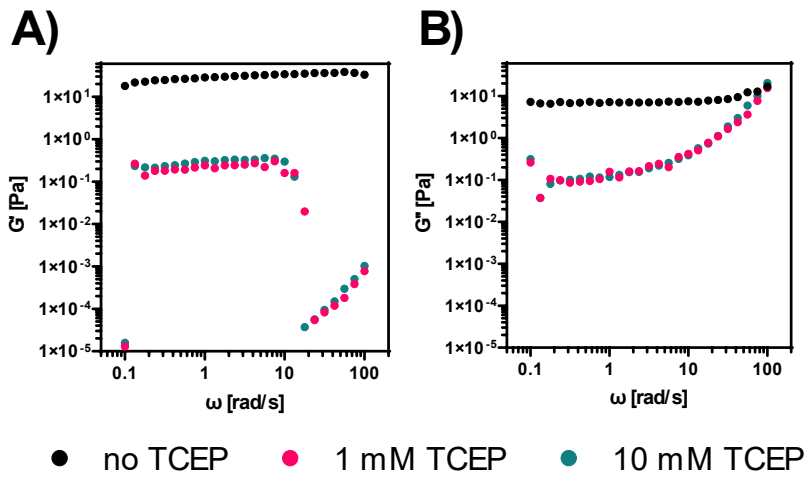


**Figure S19.** Viscoelastic properties of porcine stomach mucin at 25°C upon incubation with 1 or 10 mM TCEP in PBS pH 7.4 for 30 min at 37°C or without TCEP treatment.

## 5 FLIM Measurements

Fluorescence lifetimes of CCVJ-3D-Ahx-$N_2H_3$ were measured using a FLIM-based confocal time-correlated single photon counting setup [12] with an instrument response function (IRF) of ~100 ps (FWHM). Briefly, the fluorescence lifetime curves of CCVJ were recorded in a home-built time-correlated single photon counting (TCSPC) confocal FLIM setup [12]. The setup consists of an inverted microscope (IX71, Olympus, Shinjuku, Tokio, Japan), a tunable ps-supercontinuumwhite light laser (SuperK Extreme EXU-3, NKT Photonics, Birkerød, Denmark), a confocal scanning unit (DCS120, Becker & Hickl, Germany), a hybrid PMT detector (HPM-100-40, Becker & Hickl, Germany), and a TCSPC-module (SPC150, Becker & Hickl, Germany). FLIM images were recorded by the SPCM software (Becker & Hickl, Germany) using a 60x objective (water, UPLSAPO60XW, Olympus, Japan), resulting in a total field of view with 300 µm side length. An acousto-optical tunable filter (Select UV−VIS, NKT Photonics, Denmark) was used to select the fluorescence excitation wavelengths from the white light laser beam. The laser repetition rate was set to 19.5 MHz. CCVJ was excited at 480 nm, and the fluorescence emission was spectrally selected by a long-pass filter (>515 nm, Chroma, Rockingham, USA). A notch filter (Semrock, USA) removed the residual scattered excitation light. The TCSPC-module sorts the detected fluorescence photons into 1024 time channels with a channel width of 19.97 ps. The IRF of the system was less than 100 ps (FWHM). The maximal acquisition time of the live-cell experiments was set to 300 s. A temperature-controlled specimen holder was used and adjusted to 37 °C. Raw FLIM data were analyzed using self-written routines in C++. The fluorescence decay curve can be fitted by deconvolution of a multiexponential model function with a calculated IRF. The fitting with a multi-exponential decay function and calculation of the mean fluorescence lifetime was carried out as described in [13].

**Table S1.** Results of Fitting the Fluorescence Decays with $I(t) = \sum_{i=1}^{3} \alpha_i \, e^{-t/\tau_3}$

| | $a_1$ (%) | $t_1$ (ns) | $a_2$ (%) | $t_2$ (ns) | $a_3$ (%) | $t_3$ (ns) | $t_{mean}$* (ns) |
|---|---|---|---|---|---|---|---|
| **CCVJ-3D-Ahx-$N_2H_3$ in PBS pH 7.4** | 98.1 | **0.04** | 1.3 | **0.49** | 0.6 | **1.70** | **0.37** |
| **CCVJ-3D-Ahx-$N_2H_3$ on A549** | 65.2 | **0.32** | 25.0 | **1.33** | 9.9 | **3.47** | **1.92** |
| **CCVJ-3D-Ahx-$N_2H_3$ on A549 + 100 µM TCEP** | 69.6 | **0.33** | 26.9 | **1.28** | 3.5 | **3.32** | **1.31** |

*The mean population-weighted fluorescence lifetimes were calculated as $\tau_{mean} = \sum_{i=1}^{3} \beta_i \, \tau_i$, with $\beta_i = \frac{\alpha_i \tau_i}{\sum_i^n \alpha_i \tau_i}$.

After labelling with CCVJ-3D-Ahx-hydrazide, the mean fluorescence intensity per cell increases significantly (Fig. 5A), and the mean fluorescence lifetime is thus predominantly determined by CCVJ. Of note, the lifetime of CCVJ emission on the cell (1.8 ± 0.2 ns) is much longer than the lifetime measured in highly viscous glycerol, which is in the picosecond range.[14] This might be attributed to the additional contribution of interactions with glycans induced upon covalent attachment. After treatment of labelled cells with TCEP, we observed a decrease in the mean fluorescence lifetime of the CCVJ-3D-Ahx-labelled cells after 90 min TCEP incubation to 1.3 ns (Fig.

5B, see also Table S1). Thus, we conclude that conjugation of CCVJ with cell surface sialic acids allows detection of changes in the glycocalyx layers that occur, for example, when cross-linking is altered.

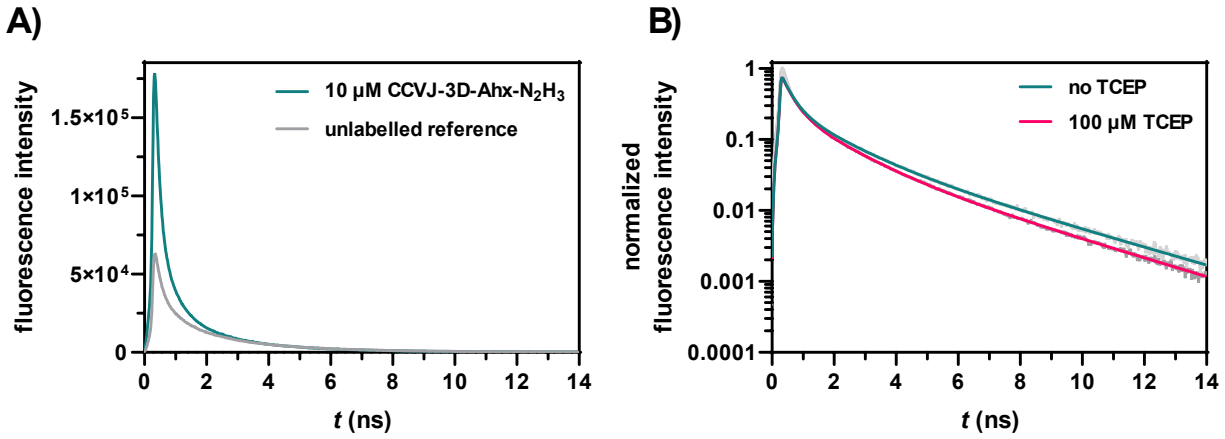


**Figure S20.** FLIM measurements of CCVJ-3D-Ahx- $N_2H_3$ bound to glycosylated structures of A549 cells. Fluorescence decay curves from the FLIM images of A) cells before and after labelling and B) cells treated with TCEP prior to labelling. Conditions: PBS pH 7.4, λex = 480 nm, λem > 515 nm long-pass filter, 37°C.

### 5.1 Mucin-labelled CCVJ-3D-Ahx-$N_2H_3$ is sensitive to Addition of Viscous Medium

The fluorescence quantum yield or fluorescence lifetime of FMR dyes increases due to steric interaction/friction, which depends on either solvent viscosity, temperature, and steric confinement (1,2). To test whether the CCVJ-3D-Ahx-$N_2H_3$ probe bound to porcine gastric mucus (PSM, Sigma) is sensitive to changes in solvent viscosity, we measured the fluorescence lifetime of PSM-CCVJ-3D-Ahx-$N_2H_3$ in buffer (PBS pH 7.4) and in 90% (w/w) glycerol solution (219 mPas). The increase in mean fluorescence lifetime from 1.61 ns to 1.70 ns proves that the mucin-bound CCVJ dye undergoes fluorescence lifetime changes depending on viscosity.

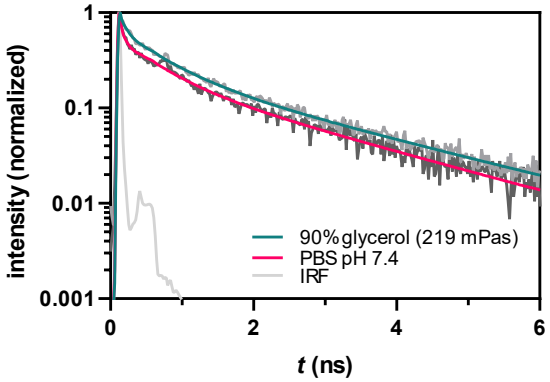


**Figure S21.** Fluorescence lifetimes of CCVJ-3D-Ahx-$N_2H_3$ were measured using a Titan-Sapphire laser-based time-correlated single photon counting setup [15] with an instrument response function (IRF) of ~30 ps (FWHM). A standard solution of fluorescein sodium salt in TRIS buffer pH 8 was measured each measurement day. The standard solution gave lifetimes within 0.01 ns accuracy. The fitting with a multi-exponential decay function and calculation of the mean fluorescence lifetime was carried out as described in [13]. Measurement condition: $\lambda_{ex}$=460nm, $\lambda_{em}$>495 nm (long pass filter GG495), 20°C.

# 6 References


1. L. Bethge, D. V. Jarikote and O. Seitz, *Bioorganic & Medicinal Chemistry*, 2008, **16**, 114-125.
2. D. Boeglin and W. D. Lubell, *Journal of Combinatorial Chemistry*, 2005, **7**, 864-878.
3. R. B. Merrifield, *Journal of the American Chemical Society*, 1963, **85**, 2149-2154.
4. E. Atherton, H. Fox, D. Harkiss, C. Logan, R. Sheppard and B. Williams, *Journal of the Chemical Society, Chemical Communications*, 1978, 537-539.
5. A. Homer and O. Seitz, *Synthesis*, 2023, DOI: 10.1055/a-2111-2333.
6. J. Schindelin, I. Arganda-Carreras, E. Frise, V. Kaynig, M. Longair, T. Pietzsch, S. Preibisch, C. Rueden, S. Saalfeld, B. Schmid, J.-Y. Tinevez, D. J. White, V. Hartenstein, K. Eliceiri, P. Tomancak and A. Cardona, *Nature Methods*, 2012, **9**, 676-682.
7. Y. Zeng, T. N. C. Ramya, A. Dirksen, P. E. Dawson and J. C. Paulson, *Nature Methods*, 2009, **6**, 207-209.
8. P. Crisalli and E. T. Kool, *The Journal of Organic Chemistry*, 2013, **78**, 1184-1189.
9. J.-Y. Tinevez, N. Perry, J. Schindelin, G. M. Hoopes, G. D. Reynolds, E. Laplantine, S. Y. Bednarek, S. L. Shorte and K. W. Eliceiri, *Methods*, 2017, **115**, 80-90.
10. D. Ershov, M.-S. Phan, J. W. Pylvänäinen, S. U. Rigaud, L. Le Blanc, A. Charles-Orszag, J. R. W. Conway, R. F. Laine, N. H. Roy, D. Bonazzi, G. Duménil, G. Jacquemet and J.-Y. Tinevez, *Nature Methods*, 2022, **19**, 829-832.
11. C. Stringer, T. Wang, M. Michaelos and M. Pachitariu, *Nature Methods*, 2021, **18**, 100-106.
12. P. Volz, R. Brodwolf, C. Zoschke, R. Haag, M. Schäfer-Korting and U. Alexiev, *Zeitschrift für Physikalische Chemie*, 2018, **232**, 671-688.
13. K. Ober, P. Volz-Rakebrand, J. Stellmacher, R. Brodwolf, K. Licha, R. Haag and U. Alexiev, *Langmuir*, 2019, **35**, 11422-11434.
14. C. Rumble, K. Rich, G. He and M. Maroncelli, *The Journal of Physical Chemistry A*, 2012, **116**, 10786-10792.
15. T.-Y. Kim, K. Winkler and U. Alexiev, *Photochemistry and Photobiology*, 2007, **83**, 378-385.

# 7 Appendix

## 7.1 Raw Data for Imaging CCVJ/AF568 ratiometric images

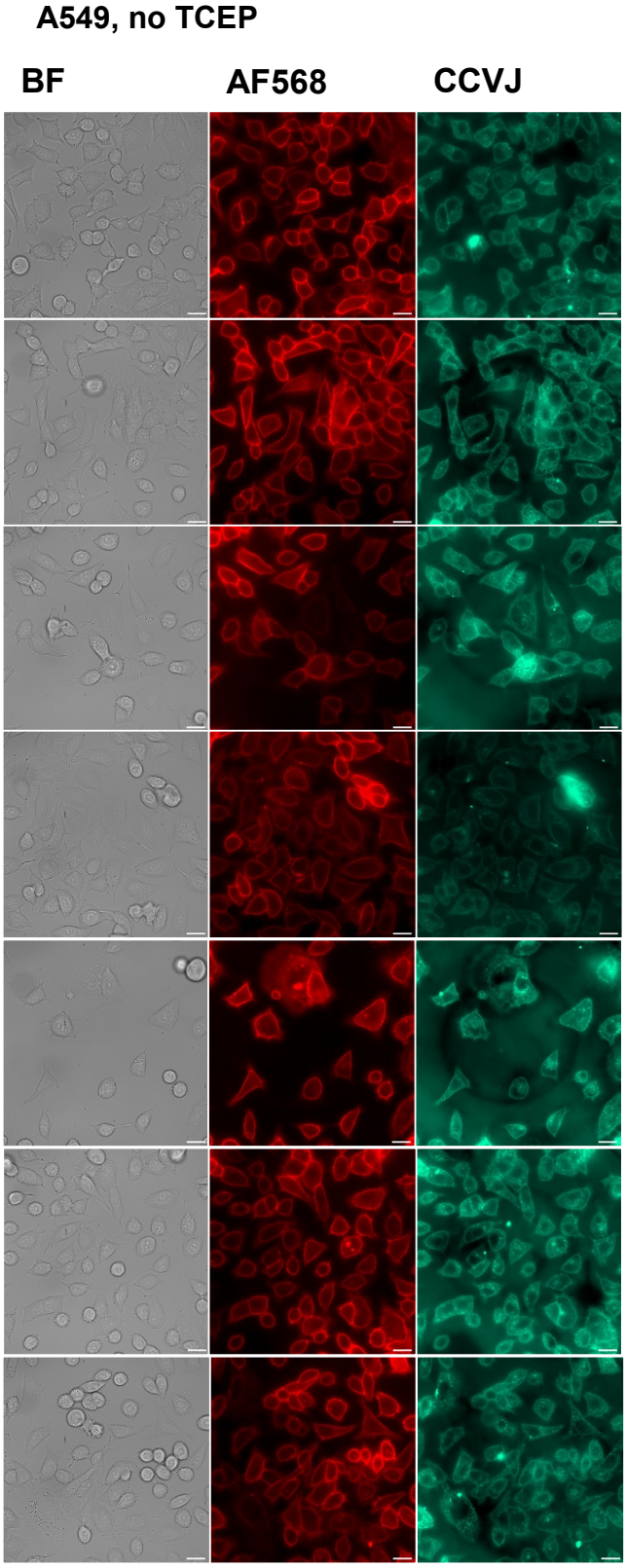


**Figure S22.** Raw image datasets (BF, AF568 and CCVJ) of A549 cells without TCEP treatment that were used for the ratiometric image analysis. Labelled with 1 µM AF568 and 10 µM CCVJ-3D-Ahx-$N_2H_3$. Scale bar = 20 µm.

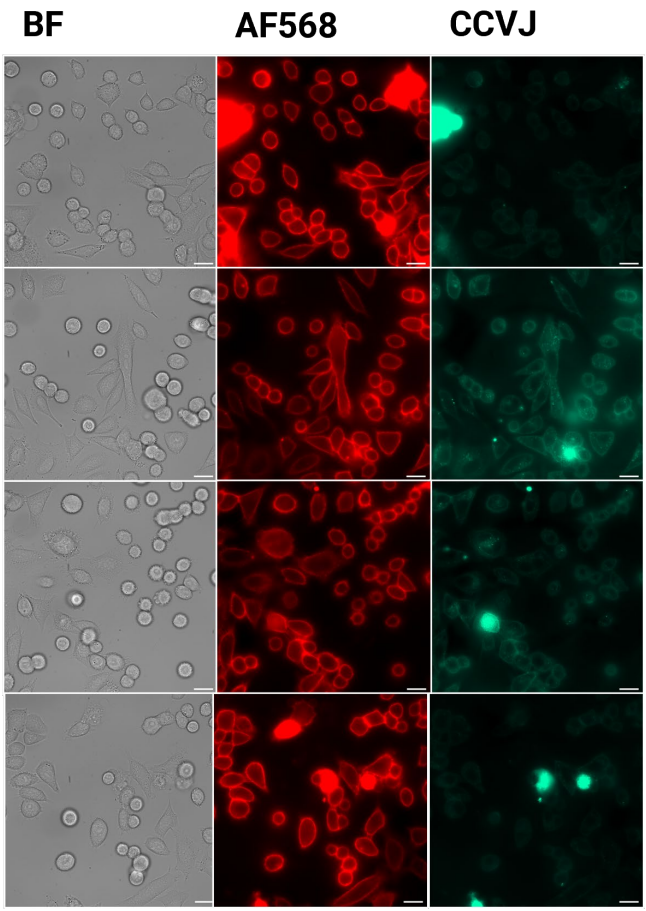


**Figure S23.** Raw image datasets (BF, AF568 and CCVJ) of A549 cells after 1h incubation at 37°C and 5% $CO_2$ with 100 µm TCEP that were used for the ratiometric image analysis. Labelled with 1 µM AF568 and 10 µM CCVJ-3D-Ahx-$N_2H_3$. Scale bar = 20 µm.

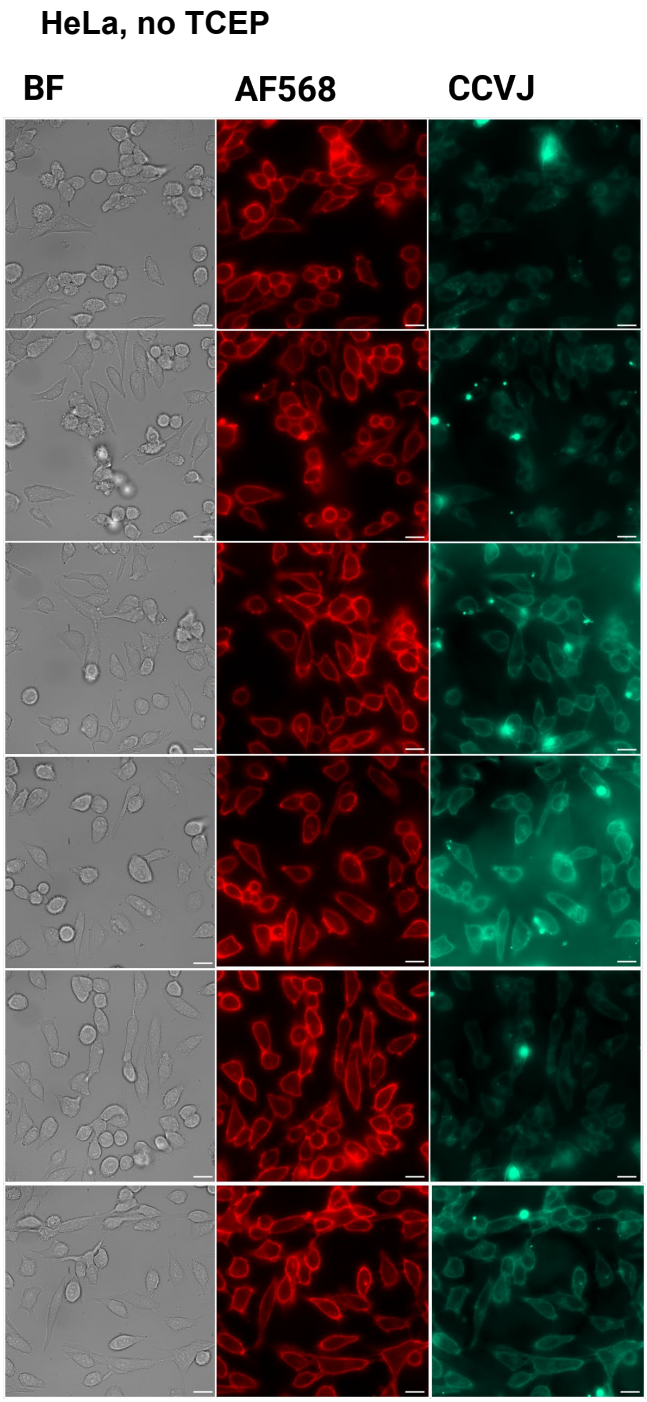


**Figure S24.** Raw image datasets (BF, AF568 and CCVJ) of HeLa cells without TCEP treatment that were used for the ratiometric image analysis. Labelled with 1 µM AF568 and 10 µM CCVJ-3D-Ahx-$N_2H_3$. Scale bar = 20 µm.

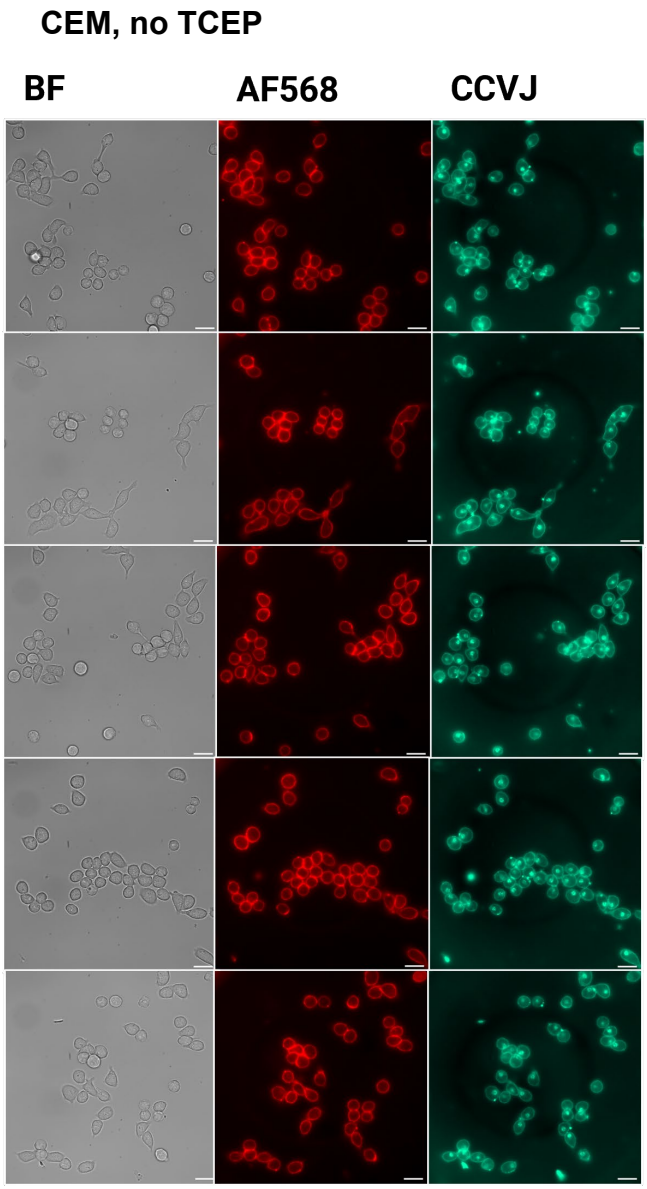


**Figure S25.** Raw image datasets (BF, AF568 and CCVJ) of CEM cells without TCEP treatment that were used for the ratiometric image analysis. Labelled with 1 µM AF568 and 10 µM CCVJ-3D-Ahx-$N_2H_3$ Scale bar = 20 µm.

### 7.2 Raw Data for Imaging TO/AF568 ratiometric images

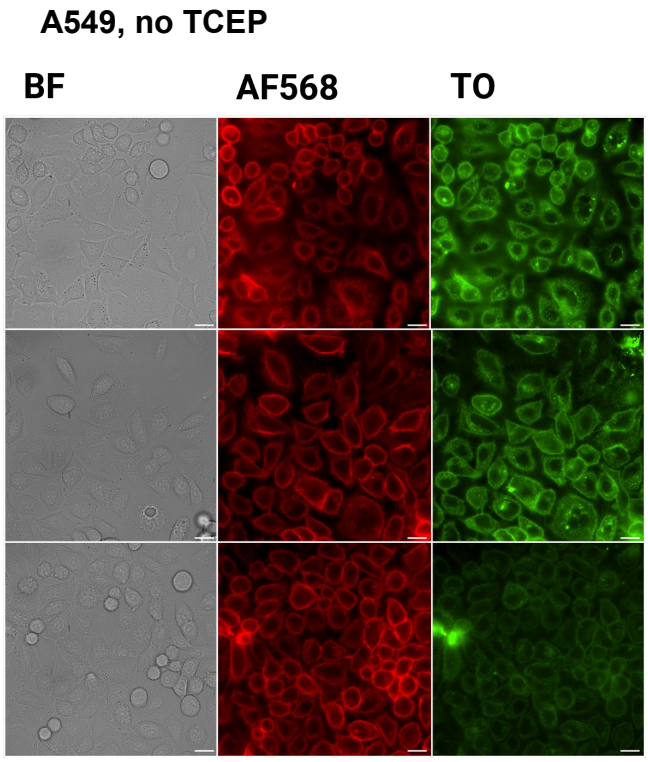


**Figure S26.** Raw image datasets (BF, AF568 and TO) of A549 cells without TCEP treatment that were used for the ratiometric image analysis. Labelled with 1 µM AF568 and 10 µM TO-3D-Ahx-$N_2H_3$. Scale bar = 20 µm.

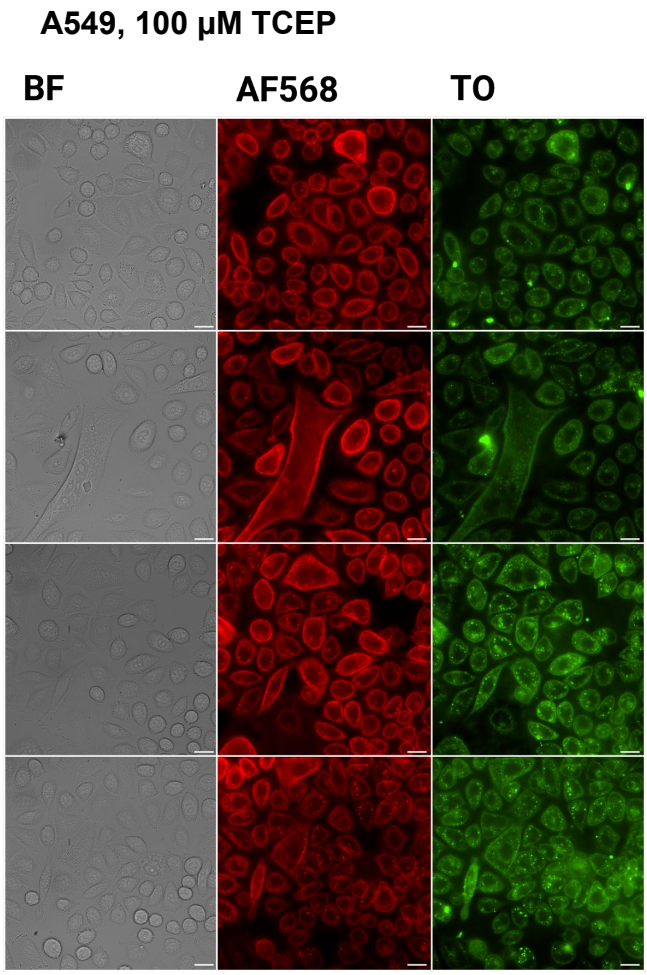


**Figure S27.** Raw image datasets (BF, AF568 and TO) of A549 cells after 1h incubation at 37°C and 5% $CO_2$ with 100 µm TCEP that were used for the ratiometric image analysis. Labelled with 1 µM AF568 and 10 µM TO-3D-Ahx-$N_2H_3$. Scale bar = 20 µm.